

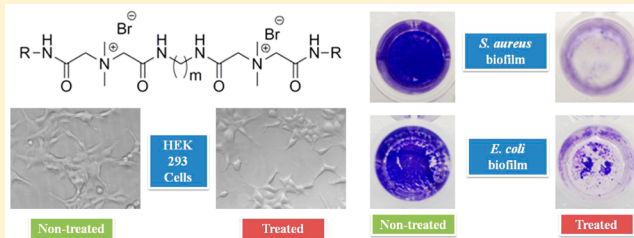
# Membrane Active Small Molecules Show Selective Broad Spectrum Antibacterial Activity with No Detectable Resistance and Eradicate Biofilms

Jiaul Hoque, Mohini M. Konai, Spandhana Gonuguntla, Goutham B. Manjunath, Sandip Samaddar, Venkateswarlu Yarlagadda, and Jayanta Haldar\*

Chemical Biology and Medicinal Chemistry Laboratory, New Chemistry Unit, Jawaharlal Nehru Centre for Advanced Scientific Research, Jakkur, Bengaluru 560064, India

## S Supporting Information

**ABSTRACT:** Treating bacterial biofilms with conventional antibiotics is limited due to ineffectiveness of the drugs and higher propensity to develop bacterial resistance. Development of new classes of antibacterial therapeutics with alternative mechanisms of action has become imperative. Herein, we report the design, synthesis, and biological evaluations of novel membrane-active small molecules featuring two positive charges, four nonpeptidic amide groups, and variable hydrophobic/hydrophilic (amphiphilic) character. The biocides synthesized via a facile methodology not only displayed good antibacterial activity against wild-type bacteria but also showed high activity against various drug-resistant bacteria such as methicillin-resistant *Staphylococcus aureus* (MRSA), vancomycin-resistant *Enterococcus faecium* (VRE), and  $\beta$ -lactam-resistant *Klebsiella pneumoniae*. Further, these biocides not only inhibited the formation of biofilms but also disrupted the established *S. aureus* and *E. coli* biofilms. The membrane-active biocides hindered the propensity to develop bacterial resistance. Moreover, the biocides showed negligible toxicity against mammalian cells and thus bear potential to be used as therapeutic agents.



## INTRODUCTION

Coupled with the inexorable proliferation of drug-resistant microorganisms, the antimicrobial drugs getting approved by the Food and Drug Administration (FDA) are declining steadily.<sup>1</sup> This poses a grim scenario for the generation to come when most antimicrobials may prove ineffective, taking human medicine to the preantibiotic era. Antibiotics, which in general target the cellular processes of bacteria, are rendered ineffective due to point mutations, production of drug-inactivating enzymes, or highly effective efflux pumps developed by bacteria.<sup>2–4</sup> Another major threat to human health is the formation of bacterial biofilms.<sup>5</sup> Pathogens living in biotic biofilms induce persistent chronic infections and significantly elevate bacterial resistance to antibiotics and the host immune system as a result of the diffusion barrier due to extracellular matrix (EPS), slow metabolism, genetic mutation, persister cells, and so on.<sup>6–8</sup> Compared with the planktonic cells, bacteria in a biofilm state are 10–1000-times more resistant to host immune responses and conventional antibiotic treatment.<sup>9–11</sup> More importantly, bacterial biofilms account for over 75% of microbial infections in humans, for example, endocarditis, periodontitis, and chronic lung infections in cystic fibrosis (CF) patients are some of the prominent diseases.<sup>11–14</sup> Furthermore, bacterial biofilms on abiotic surfaces such as implantable medical devices (e.g., urinary catheters, cardiovascular stents, etc.) play a significant role in surface-associated

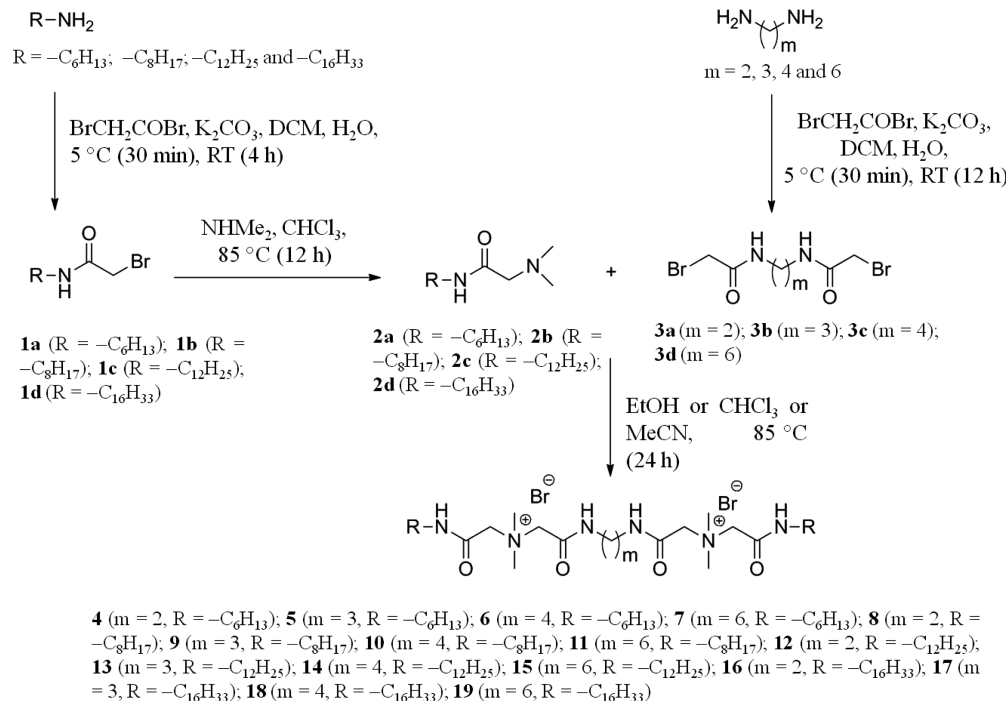
nosocomial infections in humans.<sup>15–17</sup> Therefore, searching for antibacterial agents that are not only highly active and broadly antibacterial but also able to inhibit and/or disperse bacterial biofilms and stall bacterial resistance are very essential.

Antimicrobial peptides (AMPs) and lipopeptides are Nature's very own design of membrane-active agents.<sup>18,19</sup> Cationic AMPs and lipopeptides, composed of positively charged amino acids, hydrophobic moieties from hydrophobic amino acids or fatty acids, and peptide (or amide) bonds, are known to interact with the bacterial cell membrane in a nonspecific manner.<sup>20,21</sup> Consequently, the propensity to develop bacterial resistance against these agents is low. Further, these are also shown to have the potency to destroy preformed bacterial biofilms.<sup>22,23</sup> Thus, they appear to be ideal antibacterial agents to supplement or to replace the existing antibiotic arsenal. However, low *in vivo* potency, high cost of manufacture, low stability in plasma, and low selectivity toward mammalian cells limit the large-scale use of these natural peptides as clinical antibacterial agents. Non-natural peptidomimetic approaches that mimic AMPs or lipopeptides to improve plasma stability and selectivity may circumvent the problems associated with the natural peptides. To this end, various synthetic mimics of these agents were developed such as  $\alpha$ -

Received: March 19, 2015

Published: June 23, 2015



**Scheme 1.** Synthesis of Lipophilic Cationic Small Molecular Biocides Bearing Non-peptidic Amide Groups

peptides,  $\beta$ -peptides, oligoureas, oligoacyl lysines, aryl-amide foldamers, antimicrobial polymers, alkylated peptoids, etc.<sup>24–33</sup> However, the rational design of these peptidomimetics often turns out to be complicated due to the involvement of a variety of molecular frameworks and functional groups in order to tune their structure–activity relationship and selectivity.<sup>34</sup> Furthermore, synthetic complexity associated with such molecules even limits their large-scale usage.

Recently, we have developed selective antibacterial small molecular peptidomimetics in a facile and cost-effective way based on natural and unnatural amino acids.<sup>35,36</sup> In this report, we have taken an initiative to develop highly antibacterial and nontoxic small molecules by introducing nonpeptidic amide bonds (devoid of amino acids), positive charges through quaternary ammonium groups, and hydrophobic character through a lipophilic alkyl chain using commercially available diaminoalkanes as a framework. Antibacterial activity against various bacteria and toxicity against different mammalian cells were evaluated. Also, a structure–activity relationship (SAR) was established in order to find out the effect of molecular architecture on antibacterial activity in different media. Membrane active mechanism of action, plasma stability studies, activity in the presence of complex mammalian fluids, and ability of these compounds to withstand bacterial resistance were evaluated. Further, the potential to inhibit biofilms and to destroy preformed biofilms was also evaluated in order to find the utility of these small molecules to be developed as potential antibacterial agents.

## ■ RESULTS AND DISCUSSION

**Synthesis and Characterization.** We have designed small molecules bearing two positive charges, two lipophilic moieties, and four nonpeptidic amide bonds by using diaminoalkanes, commercially available cheap starting materials, as a framework. The molecules were synthesized only in three steps (Scheme 1). In order to assess the importance of amphiphilic balance,

lipophilic alkyl chains pending from quaternary ammonium groups were varied. Further, to fine-tune the structure–activity relationship of the compounds even more, lipophilic moieties (methylene spacer) were also varied between the amine groups of the diaminoalkane frameworks. To synthesize the small molecular compounds, first various intermediates (**1a–1d**, **2a–2d**, and **3a–3d**) were prepared. Intermediates **1a–1d** were synthesized following a previously reported protocol with slight modifications.<sup>37</sup> *N*-Alkyl amines were reacted with bromoacetyl bromide in the presence of aqueous  $\text{K}_2\text{CO}_3$  to give *N*-alkyl-2-bromoethanamides (**1a–1d**, Scheme 1). The reaction was carried out at  $5^\circ\text{C}$  for 30 min (initial addition time of highly reactive bromoacetyl bromide) and then at room temperature for about 4 h to give 100% yield. Intermediates **2a–2d** were synthesized with quantitative yields by the reaction of **1a–1d** with *N,N*-dimethylamine at room temperature for 12 h and subsequent deprotonation with aqueous KOH. Another set of intermediates (**3a–3d**) was prepared following a protocol similar to the preparation of **1a–1d**. To this end, diaminoalkanes were reacted with bromoacetyl bromide to yield various reactive diamides quantitatively. Finally, the amine intermediates (**2a–2d**) were reacted individually with the diamides (**3a–3d**) to give various cationic small molecular compounds (**4–19**, Scheme 1). The products were purified and isolated by precipitation to give more than 99% yield. Different lipophilic alkyl moieties ( $\text{R} = -\text{C}_6\text{H}_{13}, -\text{C}_8\text{H}_{17}, -\text{C}_{12}\text{H}_{25}, \text{ and } -\text{C}_{16}\text{H}_{33}$ ) and lipophilic spacer moieties ( $m = 2, 3, 4, \text{ and } 6$ ) were used. Thus, a library of 16 cationic small molecules was obtained. All the final compounds were characterized by FTIR,  $^1\text{H}$  NMR,  $^{13}\text{C}$  NMR, HRMS, and elemental analyses (Figures S1–S16, Table S5, Supporting Information). Three important features of these compounds are variable hydrophobic character not only from pendent lipophilic alkyl chains but also from the lipophilic spacer chains in their design, inclusion of nonpeptidic amide bonds instead of peptide bonds formed by the conventional amino acids in AMPs or lipopeptides, and

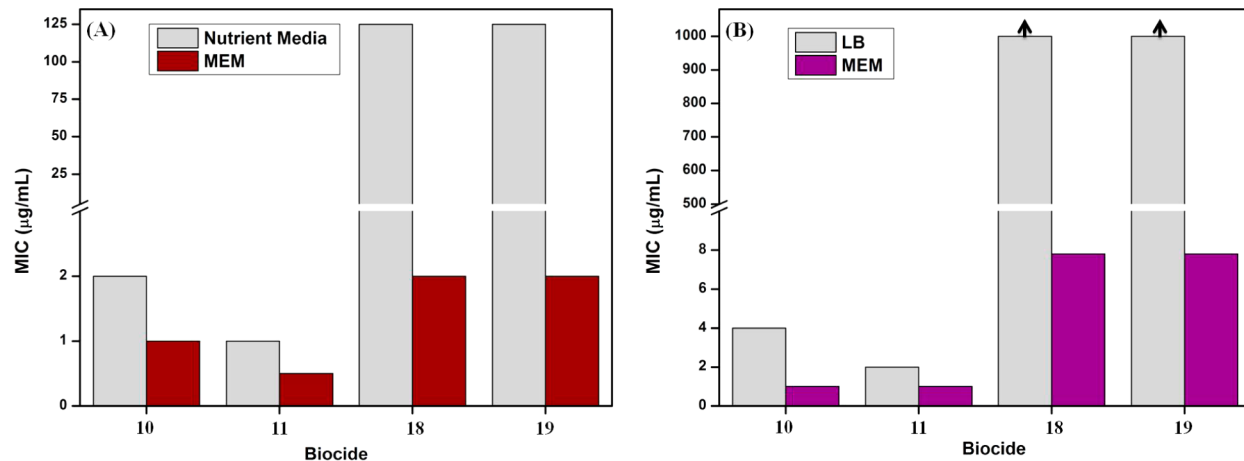


**Figure 1.** Minimum inhibitory concentrations (MICs) of cationic small molecules against (A) *S. aureus* and (B) *E. coli* in different media. Upward arrow indicates higher MIC values than the values shown.

**Table 1. Antibacterial Activity (MIC) and Hemolytic Activity ( $\text{HC}_{50}$ ) of Small Molecules**

biocides	MIC ( $\mu\text{g/mL}$ )							$\text{HC}_{50}$ ( $\mu\text{g/mL}$ )	
	drug-sensitive bacteria			drug-resistant bacteria <sup>a</sup>					
	<i>S. aureus</i>	<i>E. coli</i>	<i>P. aeruginosa</i>	MRSA	VRE	<i>K. pneumoniae</i>			
4	16	62	375	32	32	187	440		
5	16	32	187	24	24	125	420		
6	15	32	93	24	16	93	400		
7	4	24	48	8	7.8	93	338		
8	4	24	32	4	12	93	385		
9	4	12	32	4	6	48	330		
10	2	4	24	2	4	24	255		
11	0.9	2	16	1	1	16	132		
12	3.5	32	367	6	6	375	46		
13	2.8	24	367	3.9	4	375	44		
14	3.4	15.6	375	3.9	4	375	43		
15	4	31	375	3.9	4	375	41		
16	94	>1000	>1000	94	187	>1000	80		
17	94	>1000	>1000	94	187	>1000	52		
18	125	>1000	>1000	94	187	>1000	38		
19	125	>1000	>1000	125	250	>1000	36		
colistin	20	0.4	0.4	54	>199	1.2	>250		
vancomycin	0.63	b	b	0.64	750	b	>1000		

<sup>a</sup>MRSA = Methicillin-resistant *S. aureus*, VRE = vancomycin-resistant *E. faecium*, *K. pneumoniae* =  $\beta$ -lactam-resistant *Klebsiella pneumoniae*. <sup>b</sup>Not determined.

permanent positive charges from quaternary ammonium groups instead of soft charges in AMPs or lipopeptides. In order to compare the hydrophobic character of the amphiphilic molecules, retention time was measured by reverse phase high performance liquid chromatography (HPLC) for all the compounds (Figures S17–S20, Supporting Information). As expected with the increase in pending alkyl chain length, retention time increased greatly, whereas with the increase in spacer chain length, retention time increased slightly thus indicating the fine-tuning of the amphiphilic character of the compounds.

**Antibacterial Activity.** To evaluate the antibacterial efficacy, these molecules were challenged against a wide spectrum of drug-sensitive bacteria such as *S. aureus*, *E. coli*, and *P. aeruginosa* and drug-resistant bacteria such as methicillin-resistant *S. aureus* (MRSA), vancomycin-resistant *E. faecium* (VRE),  $\beta$ -lactam-resistant *K. pneumoniae*, norfloxacin-resistant

*S. aureus* (NRSA), and colistin-resistant *E. coli* (CREC). The antibacterial efficacy was determined in suitable nutrient media and expressed as minimum inhibitory concentration (MIC), that is, the minimum concentration of the molecules required to inhibit the growth of the bacteria (Figure 1, Table 1, and Tables S1–S4, Supporting Information). A glycopetide antibiotic vancomycin and a lipopeptide antibiotic colistin were also used in this study to compare the results. In general, all the compounds except 16–19 (with  $-C_{16}H_{33}$  lipophilic chain and  $m = 2–6$ ) showed good activity against all the bacteria tested in growth media. Moreover, the cationic small molecules were found to be more active toward Gram-positive bacteria than the Gram-negative bacteria. For example, the range of MIC values for the small molecules were 1–125  $\mu\text{g/mL}$  against Gram-positive *S. aureus* whereas the range of MIC values was 4–1000  $\mu\text{g/mL}$  for Gram-negative *E. coli*. However, the antibacterial activity of the cationic small molecules was found to be quite

different depending on the type of media used. For example, compound **18** (with  $-C_{16}H_{33}$  lipophilic chain and  $m = 4$ ) was found to be active in minimum essential medium ( $MIC = 3.9\text{--}7.8 \mu\text{g/mL}$ ) compared with very little or no activity in nutrient/LB media ( $MIC = 125\text{--}1000 \mu\text{g/mL}$ ) against the same bacteria.

**Effect of Lipophilic Alkyl Chain Length on Antibacterial Activity (in Nutrient Media).** Among the various sets of compounds (**4** $\text{--}$ **7** with  $-C_6H_{13}$  lipophilic chain and  $m = 2\text{--}6$ ; **8** $\text{--}$ **11** with  $-C_8H_{17}$  lipophilic chain and  $m = 2\text{--}6$ ; **12** $\text{--}$ **15** with  $-C_{12}H_{25}$  lipophilic chain and  $m = 2\text{--}6$  and **16** $\text{--}$ **19** with  $-C_{16}H_{33}$  lipophilic chain and  $m = 2\text{--}6$ ), **8** $\text{--}$ **11** were found to be most active against both Gram-positive *S. aureus* and Gram-negative *E. coli* in the growth media (Table 1). For example, the range of MIC values for compounds **8** $\text{--}$ **11** was  $1\text{--}4 \mu\text{g/mL}$  against *S. aureus* and  $2\text{--}16 \mu\text{g/mL}$  against *E. coli*, whereas the MIC values for compounds **4** $\text{--}$ **7**, **12** $\text{--}$ **15**, and **16** $\text{--}$ **19** were  $4\text{--}16 \mu\text{g/mL}$ ,  $3\text{--}4 \mu\text{g/mL}$ , and  $94\text{--}125 \mu\text{g/mL}$  against *S. aureus* and  $24\text{--}62 \mu\text{g/mL}$ ,  $16\text{--}32 \mu\text{g/mL}$ , and  $>1000 \mu\text{g/mL}$  against *E. coli*, respectively. The above results further suggested that an optimum lipophilic alkyl chain length is required for the maximum activity. To understand the role of the lipophilic alkyl chain more closely, the MIC values of the compounds of different alkyl chains (from  $-C_6H_{13}$  to  $-C_{16}H_{33}$ ) and a particular spacer chain ( $m = 6$ ) were compared. Compounds **7** ( $R = -C_6H_{13}$ ), **11** ( $R = -C_8H_{17}$ ), **15** ( $R = -C_{12}H_{25}$ ), and **19** ( $R = -C_{16}H_{33}$ ) showed MIC values of 4, 0.9, 4, and  $125 \mu\text{g/mL}$  against *S. aureus* and 24, 2, 31, and  $>1000 \mu\text{g/mL}$  against *E. coli*, respectively (Figure S21A, Supporting Information). Thus, these compounds showed a parabolic pattern with the variation lipophilic chain lengths. Interestingly, these compounds showed activity against *P. aeruginosa*, a difficult-to-treat Gram-negative bacterium that causes many nosocomial infections (hospital-acquired infections) and is known to show resistance to almost all the clinically approved drugs.<sup>38</sup> The MIC values displayed by the most active compounds **10** and **11** were 24 and  $16 \mu\text{g/mL}$ , respectively.

**Effect of Lipophilic Spacer Chain Length on Antibacterial Activity (in Growth Media).** In order to fine-tune the antibacterial activity of these small molecules further, amphiphilic balance was also varied by varying the lipophilic spacer chain length by one or two methylene units (Table 1). With the increase in lipophilic spacer length while keeping the optimum alkyl chain length constant ( $R = -C_8H_{17}$ ), antibacterial efficacy within the most active set of compounds (**8** $\text{--}$ **11**) was found to increase, for example, MIC values of **8** ( $m = 2$ ), **9** ( $m = 3$ ), **10** ( $m = 4$ ), and **11** ( $m = 6$ ) were 4, 4, 2, and  $0.9 \mu\text{g/mL}$  against *S. aureus* and 24, 12, 4, and  $2 \mu\text{g/mL}$  against *E. coli*, respectively (Figure S21B, Supporting Information). Among all the cationic small molecules, compounds **10** and **11** were found to be most active. However, irrespective of spacer chain length, compounds with  $-C_6H_{13}$  and  $-C_{16}H_{33}$  lipophilic alkyl chains were found to be less active or not active against both Gram-positive and Gram-negative bacteria in the growth media used.

**Antibacterial Activity against Drug-Resistant Bacteria (in Growth Media).** Not only active against drug-sensitive bacteria, these small molecules showed broad-spectrum activity against various drug-resistant bacteria (Table 1). Like the drug-sensitive bacteria, the cationic molecules showed similar trends in their activity against drug-resistant bacteria. The most active compounds **10** and **11** displayed MIC values of 2 and  $1 \mu\text{g/mL}$ , respectively, against MRSA. The activity of **10** and **11** against VRE was also excellent as they exhibited MIC values of 4 and 1

$\mu\text{g/mL}$ , respectively. These biocides were also found to be active against  $\beta$ -lactam-resistant *K. pneumoniae*. The MIC values of compounds **10** and **11** were 24 and  $16 \mu\text{g/mL}$ , respectively, against this Gram-negative drug-resistant bacterium. The cationic molecules were also found to be active against norfloxacin-resistant *S. aureus* (NRSA) and colistin-resistant *E. coli* (CREC). Norfloxacin and colistin, the two most common drugs used to treat the Gram-positive *S. aureus* and Gram-negative *E. coli* infections, are becoming ineffective due to the development of bacterial resistance.<sup>39,40</sup> Interestingly, compounds **10** and **11** displayed MIC values of 4 and  $2 \mu\text{g/mL}$ , respectively, against both NRSA and CREC (Table S2, Supporting Information).

**Bactericidal Activity (in Growth Media).** In order to find out whether these biocides are bacteriostatic or bactericidal or both, aliquots from the wells that appeared to have less or no turbidity in MIC experiments were plated on suitable agar plates and minimum bactericidal concentrations (MBC) were determined as the concentration where no bacterial colony was observed. Against *S. aureus*, the most active compounds **10** and **11** displayed MBC values of 4 and  $2 \mu\text{g/mL}$ , respectively. The MBC values of biocides **10** and **11** against *E. coli* were 8 and  $4 \mu\text{g/mL}$ , respectively (Table S3, Supporting Information). Overall, the excellent bactericidal activity demonstrated that these small molecular biocides might be used as potential antibacterial agents.

**Role of Medium on Antibacterial Activity.** Since the growth media used in determining MIC constitute anionic and hydrophobic peptides, interaction of the cationic small molecules with the growth media might play a major role in determining the antibacterial efficacy. In order to understand the effect of media, antibacterial efficacy of the cationic small molecules was determined in minimum essential medium (MEM), a relatively less complex medium that constitutes nonessential amino acids, sodium pyruvate, lipoic acid, vitamin B<sub>12</sub>, biotin, and ascorbic acid (Gibco, ref. 41061-029, without phenol red). Interestingly, the cationic molecules with higher lipophilic chain length (less or not active in growth media) were found to be active in MEM. For example, compound **18** (with  $-C_{16}H_{33}$  lipophilic chain and  $m = 4$ ) showed MIC values of  $2.0 \mu\text{g/mL}$  against *S. aureus* and  $7.8 \mu\text{g/mL}$  against *E. coli* in MEM, whereas the MIC values were  $125 \mu\text{g/mL}$  against *S. aureus* in nutrient medium and  $>1000 \mu\text{g/mL}$  against *E. coli* in LB medium, respectively (Figure 1, Table S3, Supporting Information). On the other hand, antibacterial activity of the small molecules with lower lipophilic chain length was found to be somewhat lower in MEM compared with the growth media. For example, compound **10** (with  $-C_8H_{17}$  lipophilic chain and  $m = 4$ ) showed MIC values of  $1.0 \mu\text{g/mL}$  each against *S. aureus* and *E. coli* in MEM, whereas the MIC values of **10** were  $2 \mu\text{g/mL}$  against *S. aureus* and  $4 \mu\text{g/mL}$  against *E. coli* in growth medium (Figure 1 and Table S2, Supporting Information). Thus, for the cationic small molecules, the nature of the medium and hence the interaction of medium with these molecules played a vital role in determining the antibacterial efficacy. This could be possibly due to the presence of mostly negatively charged and highly hydrophobic peptide residues present in peptone (an additive in nutrient media) or tryptone (an additive in LB), which resulted in strong interaction with the cationic and hydrophobic small molecules (**16** $\text{--}$ **19**) in a way that affected the antibacterial activity.<sup>41</sup>

**Antibacterial Activity in Mammalian Fluids.** One of the major disadvantages of the natural antibacterial peptides is the

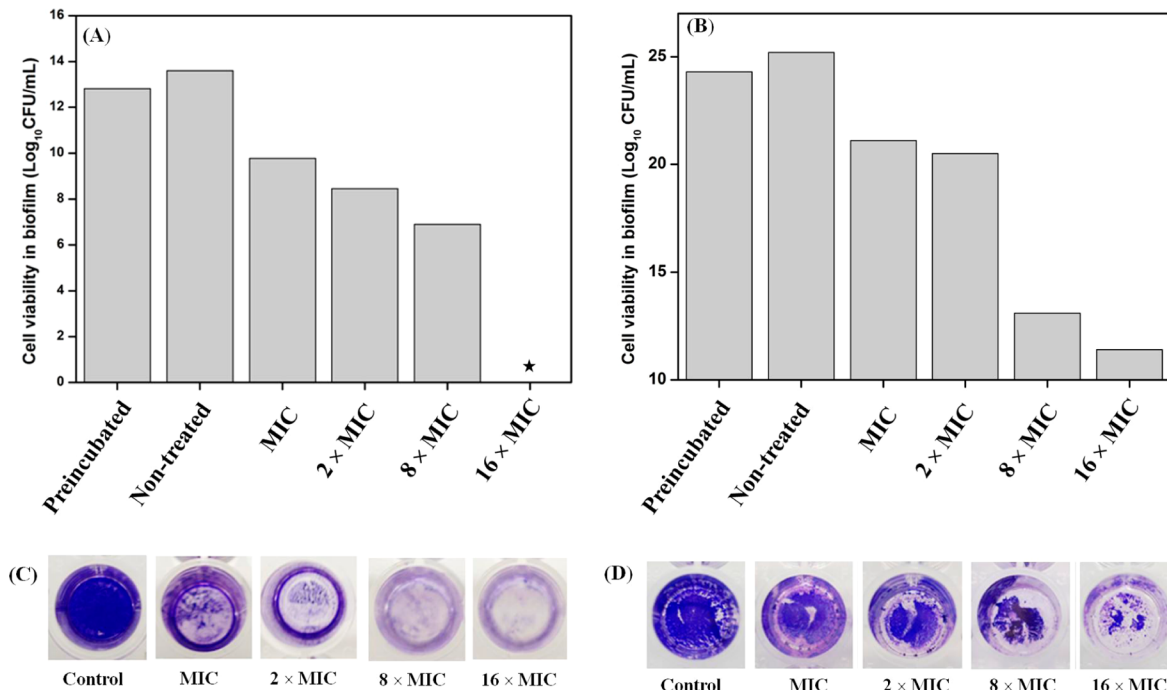


**Figure 2.** Biofilm disruption by compound **10**: (A, B) cell viability in biofilms of *S. aureus* and *E. coli*, respectively, obtained by plating and counting the viable bacteria after treating with different concentrations of the compound **10**; (C, D) images of the treated and nontreated biofilms of *S. aureus* and *E. coli*, respectively after staining with crystal violet. Star represents <50 CFU/mL.

loss of antibacterial efficacy due to protease degradation, which in turn results in decreased antibacterial activity in the blood plasma.<sup>33</sup> In order to determine the stability of the nonpeptidic amide containing biocides under plasma conditions, first these compounds were treated in 50% human plasma for different periods of time and subsequently antibacterial efficacy of the plasma-treated biocides was evaluated. The biocide used was **10** against *S. aureus*. Interestingly compound **10**, after treatment with 50% plasma for 0, 3 and 6 h did not reveal any significant loss in activity. The MIC values of **10** were found to be 2  $\mu$ g/mL each after 0 and 3 h treatment and 3  $\mu$ g/mL after 6 h treatment, respectively in 50% plasma (Figure S22A, Supporting Information). Notably, MSI-78, a naturally occurring antimicrobial peptide, is known to show 2-fold increase in MIC in the presence of 50% human serum itself than in the absence of serum (100% media).<sup>42</sup> The above result thus indicated that the compound **10** did not lose antibacterial efficacy upon pretreatment in plasma.

Another serious concern of the antibacterial agents is the loss of antibacterial activity in the presence of complex mammalian fluids.<sup>43</sup> Hence the antibacterial efficacy of these compounds was directly investigated in various complex mammalian fluid systems (50% serum, 50% plasma, and 50% blood) against MRSA, a drug-resistant Gram-positive bacterium that causes many infections in humans. Antibacterial activity was investigated by determining the minimum bactericidal concentration (MBC) of the compound **10** in 50% serum, 50% plasma, and 50% blood supplemented with 50% minimum essential media (MEM) containing  $10^5$  CFU/mL of MRSA. The compound was found to be active in 50% serum, 50% plasma, and 50% blood. The MBC values of **10** were 4  $\mu$ g/mL in 50% serum and 8  $\mu$ g/mL each in 50% plasma and 50% blood, respectively (Figure S22B, Supporting Information). The above results indicated that the compound was able to retain its antibacterial activity even in very complex mammalian

fluids like serum, plasma, and blood, thus implying its potential as an antibacterial agent. The 2–4-fold increase of MBC value could be possibly due to negatively charged proteins and macromolecules in human serum, plasma, or blood that tightly bind to the cationic molecule, thereby deactivating it toward membrane disruption of bacteria.<sup>41,43</sup>

**Antibacterial Kinetics.** Since these compounds are bactericidal in nature, the rate of bactericidal action was investigated toward both *S. aureus* and *E. coli* using compound **10** at two different concentrations (MIC and 6 × MIC). The compound showed rapid bactericidal activity against both types of bacteria. It killed *S. aureus* (~5 log reduction) at 120 min at 6 × MIC, whereas it showed bacteriostatic effect at MIC. On the other hand, the compound killed *E. coli* (~5 log reduction) at 240 min at 6 × MIC and remained bacteriostatic at MIC (Figure S23, Supporting Information). Interestingly, when antibacterial kinetics was performed in HEPES/glucose buffer (5 mM HEPES/5 mM glucose = 1:1), compound **10** killed both *S. aureus* and *E. coli* instantly (Figure S23, Supporting Information). Thus, the rate of bactericidal activity was also found to be dependent on the nature of medium.

**Antibiofilm Activity.** Bacteria within biofilms are inherently insensitive to antiseptics, microbicides, and antimicrobial peptides or defensive cells derived from the host. Further, they are 10–1000-fold more resistant to conventional antibiotic treatment.<sup>11</sup> More importantly, biofilms account for more than 80% of microbial infections in humans and thus pose a considerable impediment to antimicrobial therapy.<sup>5–8</sup> Both Gram-positive *S. aureus* and Gram-negative *E. coli* form biofilms and are known to cause many infection in humans. *S. aureus* biofilms are known cause dental caries, musculoskeletal infections, penile prostheses, and various other nosocomial infections from sutures, catheters, contact lenses, etc., whereas *E. coli* biofilms cause urinary tract infections, bacterial prostatitis, etc.<sup>5</sup> Hence we decided to evaluate

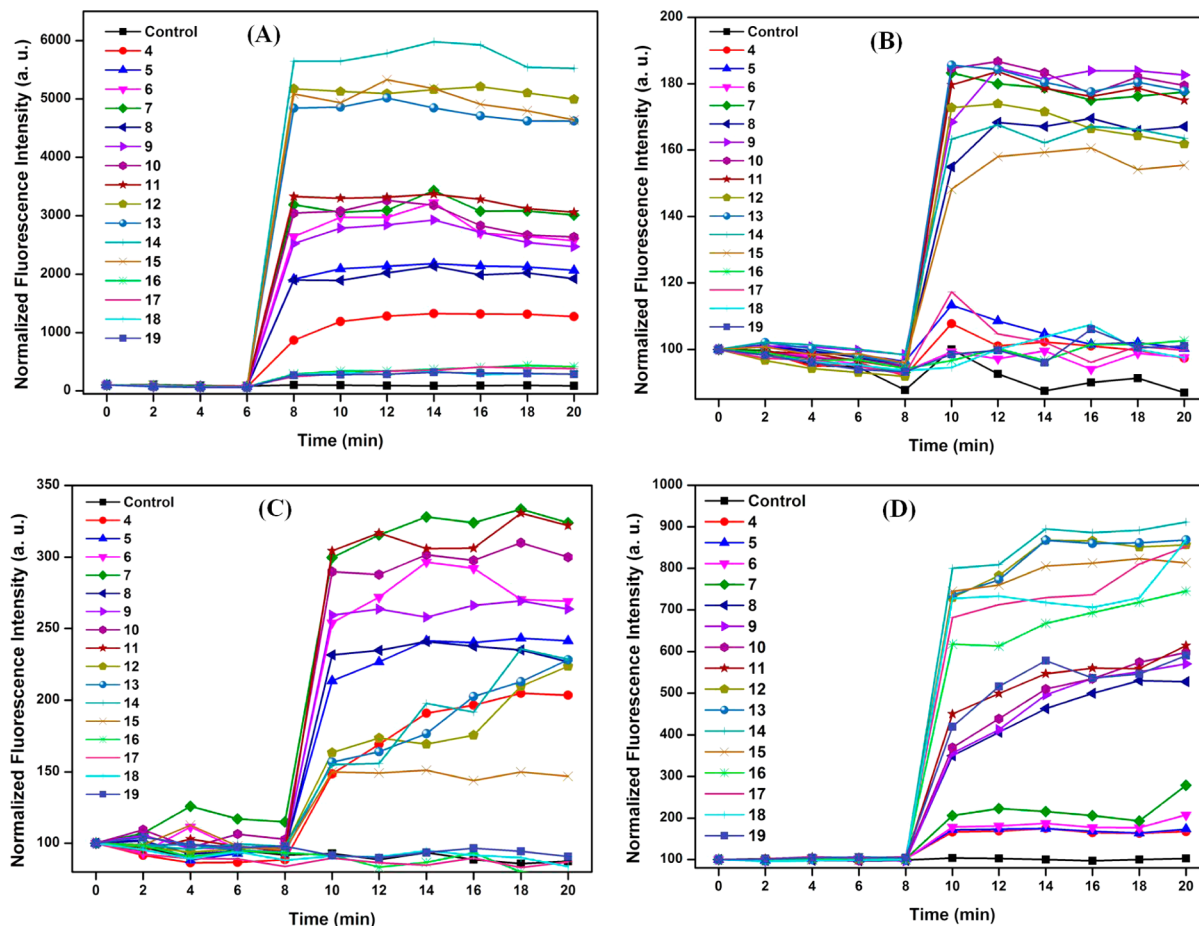


**Figure 3.** Mechanism of antibacterial action of the cationic small molecular biocides at 40  $\mu\text{g}/\text{mL}$ : (A, B) membrane depolarization against *S. aureus* and *E. coli*, respectively, using diSC3(5) dye as fluorescence probe and (C, D) cytoplasmic membrane permeabilization against *S. aureus* and *E. coli*, respectively, using propidium iodide (PI) as fluorescence probe.

the ability of these compounds to inhibit both *S. aureus* and *E. coli* biofilm formation. Further, the ability of these molecules to disperse established *S. aureus* and *E. coli* biofilms was also investigated.

**Biofilm Inhibition.** The ability of the cationic biocides to inhibit the formation of bacterial biofilm was investigated with one of the most potent biocides, **10**, against both *S. aureus* and *E. coli*. Compound **10** was found to be an effective inhibitor of both *S. aureus* and *E. coli* biofilm formation. The IC<sub>50</sub> (the concentration of the compounds that inhibits 50% biofilm development<sup>44</sup>) values of **10** against *S. aureus* and *E. coli* biofilm formation were found to be 2 and 4  $\mu\text{g}/\text{mL}$ , respectively (Figure S24, Supporting Information). Moreover, the compound at the above concentrations was found to be nonbactericidal. Thus, the ability to inhibit the biofilm formation by these biocides makes them promising antibiofilm agents.

**Biofilm Disruption.** Any antibacterial agent having the potency not only to inhibit bacterial biofilm formation but also to disperse or eradicate established biofilms would be an ideal agent to tackle infections caused by bacteria. In order to evaluate the efficiency of this class of compounds to eradicate preformed biofilms, one of the best compounds, **10**, was used against established *S. aureus* and *E. coli* biofilms. Matured *S. aureus* biofilm (developed for 24 h) having an initial count of 12.8 log<sub>10</sub> CFU/mL of bacteria was treated at four different concentrations (2, 4, 16, and 32  $\mu\text{g}/\text{mL}$ ). After the treatment,

the cell viabilities in biofilms decreased to 9.77, 8.45, and 6.9 log<sub>10</sub> CFU/mL at 2, 4, and 16  $\mu\text{g}/\text{mL}$  and to 0 at 32  $\mu\text{g}/\text{mL}$ , whereas cell viability in nontreated biofilm increased to 13.6 log<sub>10</sub> CFU/mL. Thus, the EC<sub>50</sub> (the concentration of compound that reduces 50% bacterial titer of a preformed biofilm) value of the biocide was 16.8  $\mu\text{g}/\text{mL}$ . More importantly, the biocide at the highest tested concentration (32  $\mu\text{g}/\text{mL}$ ) showed zero cell viability in 24 h *S. aureus* biofilm indicating complete eradication of established biofilm (Figure 2A). Matured *E. coli* biofilm (developed for 72 h) having an initial count of 22.5 log<sub>10</sub> CFU/mL of bacteria was similarly treated at four different concentrations (4, 8, 32, and 64  $\mu\text{g}/\text{mL}$  respectively). After the treatment, the cell viabilities in biofilms for the different concentrations decreased to 21.1, 20.5, 13.1, and 11.4 log<sub>10</sub> CFU/mL at 4, 8, 32, and 64  $\mu\text{g}/\text{mL}$  respectively (Figure 2B). Thus, the EC<sub>50</sub> value compound **10** was 63.4  $\mu\text{g}/\text{mL}$ . Moreover, the compound was able to reduce viable bacteria even in 72 h grown matured *E. coli* biofilm. The above results thus indicated the ability of the biocide to disperse the biofilms and hence to kill the microorganism present in the biofilm. The disruption of bacterial biofilms at different concentrations was also evident from the crystal violet staining of the treated biofilms (Figure 2C,D for *S. aureus* and *E. coli*, respectively).

**Mechanism of Action.** To confirm that these cationic small molecular biocides act by disrupting the bacterial cell membrane integrity, the detailed molecular mechanism of

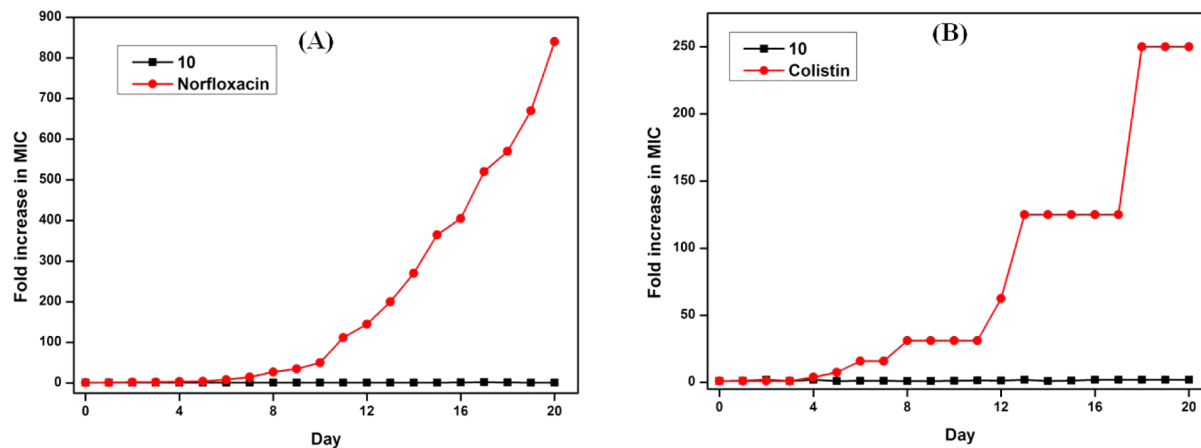


**Figure 4.** Propensity of development of bacterial resistance against compound 10: (A) for *S. aureus* where norfloxacin was used as control; (B) for *E. coli* where colistin was used as control.

action was investigated using spectroscopic methods against both Gram-positive *S. aureus* and Gram-negative *E. coli*. Also in order to assess the structure–activity relationship of the cationic biocides, membrane depolarization, intracellular potassium ion leakage, and both inner-membrane and outer-membrane permeabilization experiments were performed with all the compounds.

**Cytoplasmic Membrane Depolarization.** To find out whether the biocides act by depolarizing the bacterial cell membrane and to establish the effect of molecular architecture on membrane depolarization, fluorescence spectroscopy was used with the membrane-potential sensitive dye 3,3'-dipropylthiadicarbocyanine iodide (diSC<sub>3</sub>5).<sup>45,46</sup> In general, due to the potential gradient, the dye is taken up by the bacteria and accumulation in the membrane led to a decrease in fluorescence intensity due to self-quenching. However, when bacteria were treated with the biocides, an increase in fluorescence intensity was observed due to the displacement of diSC<sub>3</sub>5 into the solution against both *S. aureus* and *E. coli*. Thus, the above fact indicated that the biocides dissipated the membrane potential of both types of bacteria. Further, different biocides showed different extent of dissipation of membrane potential. Biocides 8–11 ( $m = 2–6$  and  $R = -C_8H_{17}$ ) and 12–15 ( $m = 2–6$  and  $R = -C_{12}H_{25}$ ) showed the maximum membrane depolarization, whereas biocides 4–7 ( $m = 2–6$  and  $R = -C_6H_{13}$ ) and 16–19 ( $m = 2–6$  and  $R = -C_{16}H_{33}$ ) exhibited less or negligible membrane depolarization against both *S. aureus* and *E. coli* (Figure 3A,B). The above results further indicated that the biocides with  $-C_8H_{17}$  and  $-C_{12}H_{25}$  lipophilic moiety are more active in disrupting the potential than the biocides with  $-C_6H_{13}$  and  $-C_{16}H_{33}$ , which are well correlated with their MIC values.

**Intracellular K<sup>+</sup> Ion Leakage.** Upon disruption of membrane potential, the intracellular potassium ion is released for both Gram-positive and Gram-negative bacteria.<sup>47</sup> Thus, the leakage of K<sup>+</sup> ions was studied using potassium ion sensitive dye PBFI-AM against both *S. aureus* and *E. coli* by fluorescence spectroscopy. PBFI-AM is known to show an increase in fluorescence after binding to K<sup>+</sup> ions if K<sup>+</sup> ions leak out from the cells. However, no increase in fluorescence intensity was observed thus indicating that none of the biocides caused significant leakage of K<sup>+</sup> ions against both types of bacteria, whereas valinomycin, used as positive control, showed K<sup>+</sup> ion leakage (Figure S25, Supporting Information).

**Outer Membrane (OM) Permeabilization.** Hydrophobic dye N-phenyl naphthylamine (NPN) is generally excluded from the OM of Gram-negative bacteria. When the OM is ruptured or damaged, NPN partitions into the perturbed OM, exhibiting an increase in fluorescence.<sup>35</sup> Upon addition of the cationic biocides, *E. coli* suspensions in the presence of NPN showed increased fluorescence. Thus, the above result indicated that *E. coli* outer membrane was damaged by the cationic biocides. Moreover, all the biocides showed outer membrane permeabilization (Figure S26, Supporting Information). Surprisingly, biocides 16–19 ( $m = 2–6$  and  $R = -C_{16}H_{33}$ ) also showed OM permeabilization at 40  $\mu$ g/mL (MIC values in LB broth of these biocides were  $\geq 1000$   $\mu$ g/mL). Since the MIC experiment was performed in LB broth, which is composed of negatively charged and hydrophobic peptides, the interaction of these cationic and hydrophobic molecules inhibited interaction with bacteria in such medium as explained earlier. Thus, compounds 16–19 being less or not active in LB medium showed membrane permeabilization in buffer solution. In order to confirm further, antibacterial activity (MBC) of compounds 11 and 18 having lower and higher lipophilic chain lengths, respectively, was determined in both buffer and LB broth at different time intervals (1, 2, 4, and 6 h). Notably, compound 18 showed activity in buffer solution (Table S4, Supporting Information).

**Inner Membrane (IM) Permeabilization.** The ability of biocides to permeabilize the cytoplasmic membrane of bacteria was studied using propidium iodide (PI) dye. PI enters inside bacteria only through compromised membranes and fluoresces upon binding to the cellular DNA.<sup>36</sup> Upon treatment with the biocides, an enhancement in the fluorescence intensity was observed in *S. aureus* and *E. coli*. Thus, the biocides were efficient in permeabilizing the cytoplasmic membranes of both Gram-positive (*S. aureus*) and Gram-negative (*E. coli*) bacteria. All the biocides were found to show the membrane permeabilization against both bacteria. Biocides 8–11 and 12–15 showed the maximum membrane permeabilization, whereas biocides 4–7 and 16–19 exhibited less or negligible membrane permeabilization against *S. aureus* (Figure 3C), which is well correlated with their MIC values. Against *E. coli*, all the biocides showed membrane permeabilization at the tested concentrations. However, biocides 16–19 along with the active molecules 8–11 and 12–15 also showed cytoplasmic permeabilization (Figure 3D) probably due to similar reason as

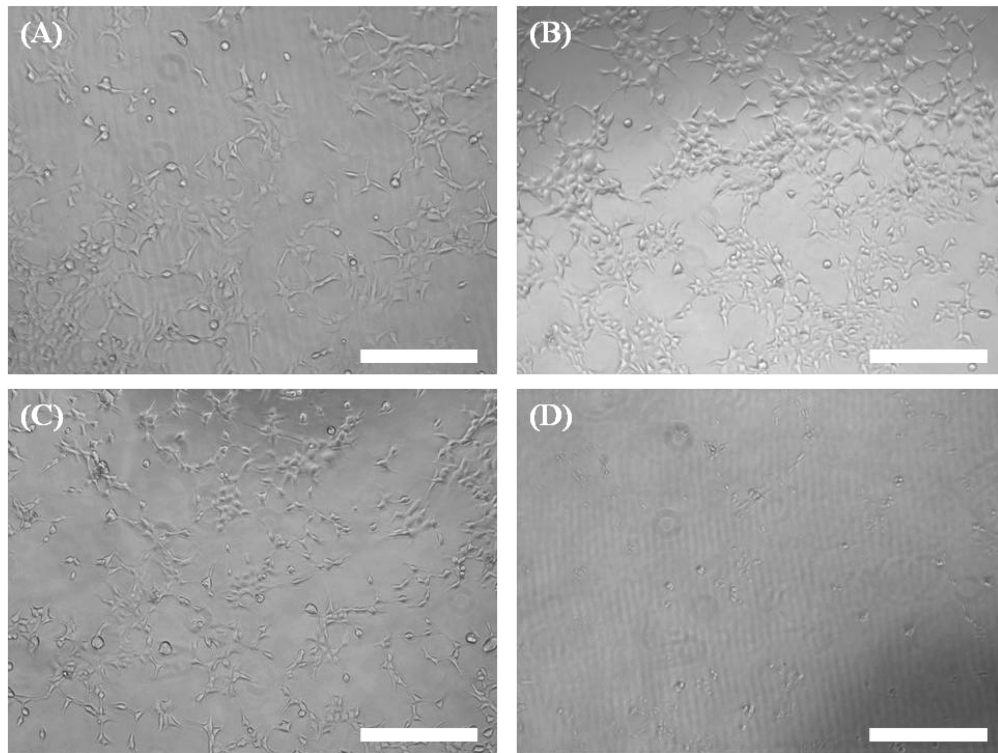


**Figure 5.** Microscopy images of HEK 293 cells: (A) cells without any treatment (control); (B) cells treated with compound **10** at 2  $\mu\text{g}/\text{mL}$ ; (C) cells treated with **10** at 24  $\mu\text{g}/\text{mL}$ , and (D) cells treated with triton-X (1 vol %). Scale bar 20  $\mu\text{m}$ .

explained earlier. In summary, all the above studies indicated that these cationic small molecules indeed interacted with the negatively charged bacterial cell membrane and disrupted the membrane integrity.

**Propensity To Induce Bacterial Resistance.** The development of bacterial resistance against most of the clinically approved drugs is one of the major problems of current times.<sup>1–3</sup> Thus, it would be of importance to evaluate the potential emergence of bacterial resistance against these biocides. The ability of these biocides to suppress the development of resistance was evaluated by taking one of the most active biocides (**10**) against both Gram-positive *S. aureus* and Gram-negative *E. coli*.<sup>47,48</sup> Norfloxacin, an antibiotic commonly used to treat the Gram-positive infections, was used as a positive control for *S. aureus*, whereas colistin, a lipopeptide antibiotic active against Gram-negative bacteria, was used in the case of *E. coli*. These antibacterial agents were repeatedly challenged against bacteria at their sub-MIC values to allow bacteria to develop resistance. Interestingly, no change in the MIC of **10** was observed against both *S. aureus* and *E. coli* even after 20 passages, whereas around 810-fold and 248-fold increase in MIC was observed in case of norfloxacin and colistin, respectively (Figure 4). The above results thus indicated that bacteria find it difficult to develop resistance against this type of biocide within the experimental time period.

**Cytotoxicity against Mammalian Cells.** One of the major concerns in the development of clinically useful antibacterial agents for biomedical applications is their selectivity toward mammalian cells over bacterial cells. In order to evaluate the cytotoxic effect, hemolytic activity against human erythrocytes as well as cytotoxicity against human embryonic kidney (HEK) cells and human cervical cancer derived HeLa cells were performed.<sup>49,50</sup>

**Hemolytic Activity.** The ability of the small molecular biocides to lyse human red blood cells (hRBC) was expressed as  $\text{HC}_{50}$  ( $\mu\text{g}/\text{mL}$ ), that is, the concentration of the biocides at which 50% of RBC gets lysed (Figure S27, Supporting Information). In general, hemolytic activity was found to increase with the increase in liphophilic chain length pending from quaternary nitrogen (Table 1). For example, the  $\text{HC}_{50}$  values of compounds **4** ( $m = 2$  and  $R = -\text{C}_6\text{H}_{13}$ ), **8** ( $m = 2$  and  $R = -\text{C}_8\text{H}_{17}$ ), **12** ( $m = 2$  and  $R = -\text{C}_{12}\text{H}_{25}$ ) and **16** ( $m = 2$  and  $R = -\text{C}_{16}\text{H}_{33}$ ) were 440, 385, 66, and 52  $\mu\text{g}/\text{mL}$ , respectively. On the other hand, with the increase in lipophilic spacer chain length, the hemolytic activity was found to increase but to a lesser extent. For example, the  $\text{HC}_{50}$  values of compounds **4** ( $m = 2$  and  $R = -\text{C}_6\text{H}_{13}$ ), **5** ( $m = 3$  and  $R = -\text{C}_6\text{H}_{13}$ ), **6** ( $m = 4$  and  $R = -\text{C}_6\text{H}_{13}$ ), and **7** ( $m = 6$  and  $R = -\text{C}_6\text{H}_{13}$ ) were 440, 420, 400, and 338  $\mu\text{g}/\text{mL}$ , respectively. However, compound **10**, one of the most potent biocides, showed  $\text{HC}_{50}$  value of 255  $\mu\text{g}/\text{mL}$  thus giving selectivity ( $S = \text{HC}_{50}/\text{MIC}$ ) of 128 and 64 against *S. aureus* and *E. coli* respectively (Table 1). Compound **10** showed no hemolytic activity at 4  $\mu\text{g}/\text{mL}$  and 1–2% hemolysis at 40  $\mu\text{g}/\text{mL}$  (at MIC and 10  $\times$  MIC values for *E. coli* and most of the drug-resistant bacteria). The above results thus indicated that these compounds are selectively active toward bacteria.

**Cytotoxicity.** To strengthen the selectivity of the cationic biocides, cytotoxicity study was also performed with HEK 293 and HeLa cells by optical microscopy. Cells were treated with the biocides **10** and **11** at lowest and highest MIC values (2 and 24  $\mu\text{g}/\text{mL}$  for **10** and 1 and 16  $\mu\text{g}/\text{mL}$  for **11**), and the treated cell lines were imaged to visualize the morphology (Figure 5, Figures S28–S30, Supporting Information). The biocide treated cells were found to have spindle shape with intact morphology at both concentrations and were similar to the

untreated cell lines (Figure 5A–C), whereas cells treated with triton-X were found to have completely irregular shape and damaged morphology (Figure 5D). These results thus indicated that these biocides are indeed nontoxic toward mammalian cells at their MIC values.

## CONCLUSION

In conclusion, novel membrane-active small molecules have been developed via simple yet quantitative methodology. The compounds displayed excellent antibacterial activity against various wild-type and drug-resistant bacteria (both Gram-positive and Gram-negative). Variation of amphiphilic nature of the compounds drastically improved their antibacterial activity as well as selectivity. Additionally, the small molecules were found to be stable under plasma conditions and showed excellent activity in various complex mammalian fluids such as serum, plasma, and blood. Further, these compounds not only inhibited the formation of biofilm but also dispersed the established bacterial biofilms. These molecules acted on bacteria rapidly by disrupting the membrane and did not allow bacteria to develop resistance. The compounds showed negligible toxicity against mammalian cells. Thus, the membrane-active small molecules developed herein could be used as therapeutic agents to treat bacterial infections caused by multidrug-resistant bacteria in both planktonic and biofilm state.

## EXPERIMENTAL SECTION

**Materials and Instrumentation.** 1-Aminohexane, 1-aminoctane, 1-aminododecane, 1-aminohexadecane, bromoacetyl bromide, 1,2-diaminoethane, 1,3-diaminopropane, 1,4-diaminobutane, 1,6-diaminohexane, 2-[4-(2-hydroxyethyl)piperazin-1-yl]ethanesulfonic acid (HEPES), and  $\alpha$ -D(+)-glucose were purchased from Sigma-Aldrich and used as received. Anhydrous potassium carbonate ( $K_2CO_3$ ), anhydrous sodium sulfate ( $Na_2SO_4$ ), phosphorus pentaoxide ( $P_2O_5$ ), calcium hydride ( $CaH_2$ ), *N,N*-dimethylamine solution (40%), dichloromethane (DCM), chloroform, ethanol, acetonitrile, diethyl ether, acetone, and molecular sieves (4 Å) were purchased from SD Fine, India, and were of analytical grade. Acetonitrile, DCM, and chloroform were dried over  $P_2O_5$ , and ethanol was dried over  $CaH_2$  and stored over molecular sieves. Nuclear magnetic resonance (NMR) spectra were recorded using Bruker AMX-400 (400 MHz for  $^1H$  NMR and 100 MHz for  $^{13}C$  NMR) spectrometer. The chemical shift ( $\delta$ ) values are reported in parts per million (ppm). Mass spectra were recorded on a 6538-UHD Accurate mass Q-TOF LC-MS high resolution mass spectrometer (HRMS). Infrared (IR) spectra were recorded by Bruker IFS66 V/s spectrometer on NaCl crystal for liquid compounds and KBr pellet for solid compounds. Elemental analyses were performed by a Thermo Finnigan FLASH EA 1112 CHNS analyzer. For optical density (OD) measurement, Tecan Infinite Pro series M200 microplate reader was employed. *Staphylococcus aureus* (MTCC 737) and *Escherichia coli* (MTCC 443) were purchased from MTCC (Chandigarh, India). *Pseudomonas aeruginosa* (ATCC 424), methicillin-resistant *Staphylococcus aureus* (ATCC 33591), vancomycin-resistant *Enterococcus faecium* (ATCC 51559), and  $\beta$ -lactam-resistant *Klebsiella pneumoniae* (ATCC 700603) were obtained from ATCC (Rockville, MD, USA).

**General Procedure for the Synthesis of *N*-Alkyl-2-bromoethanamides (1a–1d).** 1-Aminoalkanes (60 mmol) were dissolved in DCM (100 mL), and a solution of  $K_2CO_3$  (12.4 g, 90 mmol) in water (100 mL) was added to it. The binary mixture was then cooled to 5 °C in a cold incubator connected to a chiller. Bromoacetyl bromide (18.2 g, 90 mmol) was dissolved in DCM (75 mL) and was added to the mixture dropwise for about 30 min. After the completion of addition, the reaction mixture was stirred at room temperature for about 4 h. After the reaction, the organic layer was separated using a separating

funnel, and the aqueous layer was subjected to repeated washes with DCM (2 × 50 mL). All the organic solutions were combined and washed with water repeatedly (3 × 100 mL). The final organic layer was then passed through anhydrous  $Na_2SO_4$ . The DCM layer was collected, and the solvent was evaporated to obtain colorless liquids or solids with 100% yield. The products were characterized by FT-IR,  $^1H$  NMR, and  $^{13}C$  NMR spectroscopy.

**2-Bromo-*N*-hexylethanamide (1a).** FTIR: 3250 cm<sup>-1</sup> (amide N–H str.), 2928 cm<sup>-1</sup> (–CH<sub>2</sub>– assym. str.), 2850 (–CH<sub>2</sub>– sym. str.), 1680 cm<sup>-1</sup> (Amide I, C=O str.), 1560 cm<sup>-1</sup> (Amide II, N–H ben.), 1470 cm<sup>-1</sup> (–CH<sub>2</sub>– scissor).  $^1H$  NMR (400 MHz, CDCl<sub>3</sub>):  $\delta$  0.859 (t, terminal –CH<sub>3</sub>, 3H), 1.309 (m, -(CH<sub>2</sub>)<sub>3</sub>–, 6H), 1.530 (q, –CH<sub>2</sub>(CH<sub>2</sub>)<sub>3</sub>–, 2H), 3.248 (m, –CONHCH<sub>2</sub>–, 2H), 3.861 (s, –COCH<sub>2</sub>Br, 2H), 6.581 (br s, amide –NHCO, 1H).  $^{13}C$  NMR (100 MHz, CDCl<sub>3</sub>):  $\delta$  14.190, 22.770, 26.912, 29.711, 31.994, 40.408, 165.589.

**2-Bromo-*N*-octylethanamide (1b).** FTIR: 3252 cm<sup>-1</sup> (amide N–H str.), 2929 cm<sup>-1</sup> (–CH<sub>2</sub>–assym. str.), 2851 (–CH<sub>2</sub>– sym. str.), 1680 cm<sup>-1</sup> (Amide I, C=O str.), 1556 cm<sup>-1</sup> (Amide II, N–H ben.), 1469 cm<sup>-1</sup> (–CH<sub>2</sub>– scissor).  $^1H$  NMR (400 MHz, CDCl<sub>3</sub>):  $\delta$  0.877 (t, terminal –CH<sub>3</sub>, 3H), 1.291 (m, -(CH<sub>2</sub>)<sub>5</sub>–, 10H), 1.535 (q, –CH<sub>2</sub>(CH<sub>2</sub>)<sub>5</sub>–, 2H), 3.252 (t, –CONHCH<sub>2</sub>–, 2H), 3.865 (s, –COCH<sub>2</sub>Br, 2H), 6.565 (br s, amide –NHCO, 1H).  $^{13}C$  NMR (100 MHz, CDCl<sub>3</sub>):  $\delta$  14.188, 22.698, 26.904, 29.411, 29.589, 29.998, 31.989, 40.402, 165.578.

**2-Bromo-*N*-dodecylethanamide (1c).** FT-IR: 3251 cm<sup>-1</sup> (amide N–H str.), 2929 cm<sup>-1</sup> (–CH<sub>2</sub>–assym. str.), 2851 (–CH<sub>2</sub>– sym. str.), 1685 cm<sup>-1</sup> (Amide I, C=O str.), 1558 cm<sup>-1</sup> (Amide II, N–H ben.), 1470 cm<sup>-1</sup> (–CH<sub>2</sub>– scissor).  $^1H$  NMR (400 MHz, CDCl<sub>3</sub>):  $\delta$  0.858 (t, terminal –CH<sub>3</sub>, 3H), 1.289 (m, -(CH<sub>2</sub>)<sub>9</sub>–, 18H), 1.533 (q, –CH<sub>2</sub>(CH<sub>2</sub>)<sub>9</sub>–, 2H), 3.278 (t, –CONHCH<sub>2</sub>–, 2H), 3.881 (s, –COCH<sub>2</sub>Br, 2H), 6.475 (br s, amide –NHCO, 2H).  $^{13}C$  NMR (100 MHz, CDCl<sub>3</sub>):  $\delta$  14.192, 22.765, 26.901, 29.321, 29.420, 29.585, 29.643, 29.705, 31.992, 40.401, 165.587.

**2-Bromo-*N*-hexadecylethanamide (1d).** FT-IR: 3250 cm<sup>-1</sup> (amide N–H str.), 2927 cm<sup>-1</sup> (–CH<sub>2</sub>– assym. str.), 2849 (–CH<sub>2</sub>– sym. str.), 1679 cm<sup>-1</sup> (Amide I, C=O str.), 1562 cm<sup>-1</sup> (Amide II, N–H ben.), 1468 cm<sup>-1</sup> (–CH<sub>2</sub>– scissor).  $^1H$  NMR (400 MHz, CDCl<sub>3</sub>):  $\delta$  0.878 (t, terminal –CH<sub>3</sub>, 3H), 1.300 (m, -(CH<sub>2</sub>)<sub>13</sub>–, 26H), 1.547 (q, –CH<sub>2</sub>(CH<sub>2</sub>)<sub>13</sub>–, 2H), 3.279 (t, –CONHCH<sub>2</sub>–, 2H), 3.883 (s, –COCH<sub>2</sub>Br, 2H), 6.575 (br s, amide –NHCO, 2H).  $^{13}C$  NMR (100 MHz, CDCl<sub>3</sub>):  $\delta$  14.193, 22.769, 26.903, 29.334, 29.413, 29.578, 29.636, 29.718, 29.818, 32.095, 40.413, 165.567.

**General Procedure for the Synthesis of 2-(*N,N*-Dimethyl)-*N'*-alkylethanamide (2a–2d).** *N*-Alkyl-1-bromoethanamides 1a–1d (40 mmol) were dissolved in dry chloroform (40 mL) in a screw-top pressure tube. Dry NHMe<sub>2</sub> gas was added to the solution of *N*-alkyl-1-bromoethanamide in chloroform at 0 °C until the volume of the resulting solution was roughly doubled (80 mL). Then the reaction mixture was stirred for 24 h at 80 °C overnight. After the reaction, the pressure tube was cooled, the reaction mixture was transferred to a round-bottom (RB) flask, and the final volume of the reaction mixture was brought to 150 mL by adding chloroform. The unreacted gas was removed carefully by heating slowly until wet litmus paper no longer turns blue on exposure to the emerging vapors. The solution was washed with 2 M KOH solution (3 × 100 mL) in order to deprotonate the products. Finally, the organic layer was passed through anhydrous  $Na_2SO_4$  and was dried to give yellow colored liquids with 100% yield. The products were characterized by FT-IR,  $^1H$  NMR, and  $^{13}C$  NMR spectroscopy.

**2-(*N,N*-Dimethyl)-*N'*-hexylethanamide (2a).** FT-IR (KBr): 3230 cm<sup>-1</sup> (amide N–H str.), 2926 cm<sup>-1</sup> (–CH<sub>2</sub>– assym. str.), 2852 cm<sup>-1</sup> (–CH<sub>2</sub>– sym. str.), 1680 cm<sup>-1</sup> (Amide I, C=O str.), 1560 cm<sup>-1</sup> (Amide II, N–H ben.), 1470 cm<sup>-1</sup> (–CH<sub>2</sub>– scissor).  $^1H$  NMR (400 MHz, CDCl<sub>3</sub>):  $\delta$  0.879 (t, terminal –CH<sub>3</sub>, 3H), 1.239 (m, CH<sub>3</sub>(CH<sub>2</sub>)<sub>3</sub>–, 6H), 1.547 (q, CH<sub>3</sub>(CH<sub>2</sub>)<sub>3</sub>CH<sub>2</sub>–, 2H), 2.286 (s, (CH<sub>3</sub>)<sub>2</sub>N–, 6H), 2.883 (s, (CH<sub>3</sub>)<sub>2</sub>NCH<sub>2</sub>CO–, 2H), 3.224 (q, –CH<sub>2</sub>NHCO–, 2H), 7.137 (br s, amide –NH, 1H).

**2-(*N,N*-Dimethyl)-*N'*-octylethanamide (2b).** FT-IR (KBr): 3232 cm<sup>-1</sup> (amide N–H str.), 2936 cm<sup>-1</sup> (–CH<sub>2</sub>– assym. str.), 2855 cm<sup>-1</sup>

( $-\text{CH}_2-$  sym. str.), 1678  $\text{cm}^{-1}$  (Amide I,  $\text{C}=\text{O}$  str.), 1560  $\text{cm}^{-1}$  (Amide II, N–H ben.), 1470  $\text{cm}^{-1}$  ( $-\text{CH}_2-$  scissor).  $^1\text{H}$  NMR (400 MHz,  $\text{CDCl}_3$ ):  $\delta$  0.831 (t, terminal  $-\text{CH}_3$ , 3H), 1.237 (m,  $\text{CH}_3(\text{CH}_2)_5-$ , 10H), 1.489 (q,  $\text{CH}_3(\text{CH}_2)_5\text{CH}_2-$ , 2H), 2.236 (s,  $(\text{CH}_3)_2\text{N}-$ , 6H), 2.884 (s,  $(\text{CH}_3)_2\text{NCH}_2\text{CO}-$ , 2H), 3.274 (q,  $-\text{CH}_2\text{NHCO}-$ , 2H), 7.139 (br s, amide  $-\text{NH}$ , 1H).

**2-(N,N-Dimethyl)-N'-dodecylethanamide (2c).** FT-IR (KBr): 3229  $\text{cm}^{-1}$  (amide N–H str.), 2934  $\text{cm}^{-1}$  ( $-\text{CH}_2-$  assym. str.), 2856  $\text{cm}^{-1}$  ( $-\text{CH}_2-$  sym. str.), 1680  $\text{cm}^{-1}$  (Amide I,  $\text{C}=\text{O}$  str.), 1559  $\text{cm}^{-1}$  (Amide II, N–H ben.), 1471  $\text{cm}^{-1}$  ( $-\text{CH}_2-$  scissor).  $^1\text{H}$  NMR (400 MHz,  $\text{CDCl}_3$ ):  $\delta$  0.869 (t, terminal  $-\text{CH}_3$ , 3H), 1.247 (m,  $\text{CH}_3(\text{CH}_2)_9-$ , 18H), 1.489 (q,  $\text{CH}_3(\text{CH}_2)_9\text{CH}_2-$ , 2H), 2.229 (s,  $(\text{CH}_3)_2\text{N}-$ , 6H), 2.926 (s,  $(\text{CH}_3)_2\text{NCH}_2\text{CO}-$ , 2H), 3.281 (q,  $-\text{CH}_2\text{NHCO}-$ , 2H), 7.136 (br s, amide  $-\text{NH}$ , 1H).

**2-(N,N-Dimethyl)-N'-hexadecylethanamide (2d).** FT-IR (KBr): 3228  $\text{cm}^{-1}$  (amide N–H str.), 2935  $\text{cm}^{-1}$  ( $-\text{CH}_2-$  assym. str.), 2859  $\text{cm}^{-1}$  ( $-\text{CH}_2-$  sym. str.), 1681  $\text{cm}^{-1}$  (Amide I,  $\text{C}=\text{O}$  str.), 1559  $\text{cm}^{-1}$  (Amide II, N–H ben.), 1470  $\text{cm}^{-1}$  ( $-\text{CH}_2-$  scissor).  $^1\text{H}$  NMR (400 MHz,  $\text{CDCl}_3$ ):  $\delta$  0.871 (t, terminal  $-\text{CH}_3$ , 3H), 1.239 (m,  $\text{CH}_3(\text{CH}_2)_{13}-$ , 26H), 1.529 (q,  $\text{CH}_3(\text{CH}_2)_{13}\text{CH}_2-$ , 2H), 2.268 (s,  $(\text{CH}_3)_2\text{N}-$ , 6H), 2.934 (s,  $(\text{CH}_3)_2\text{NCH}_2\text{CO}-$ , 2H), 3.265 (q,  $-\text{CH}_2\text{NHCO}-$ , 2H), 7.120 (br s, amide  $-\text{NH}$ , 1H).

**General Procedure for the Synthesis of Alkane Dibromoethanamide (3a–3d).** Diaminoalkanes (50 mmol) were dissolved in chloroform (100 mL), and a solution of  $\text{K}_2\text{CO}_3$  (20.7 g, 150 mmol) in water (100 mL) was added to it. The binary mixture was then cooled to 5 °C in a cold incubator. Bromoacetyl bromide (30.4 g, 150 mmol) was dissolved in chloroform (100 mL) and was added to the mixture dropwise for about 30 min. After the completion of addition, the reaction mixture was stirred at room temperature for 12 h. After the reaction, the insoluble solid was filtered through a sintered glass funnel and washed repeatedly with water. Finally, the precipitate was dried in a vacuum oven at 60 °C to obtain white colored products (1st collection). Also, the organic layer from the reaction mixture after the filtration was separated using a separating funnel, and the aqueous layer was subjected to repeated washes with chloroform (2 × 50 mL). All the organic solutions were then combined and washed with water (3 × 75 mL). The final organic layer was passed through anhydrous  $\text{Na}_2\text{SO}_4$ . The organic solvent was evaporated to obtain white products (2nd collection). The products were characterized by FT-IR,  $^1\text{H}$  NMR, and  $^{13}\text{C}$  NMR spectroscopy. The products obtained in both ways (from precipitate and solution) were the same, and their combined weight gave quantitative (100%) yield of 3a–3d.

**N,N'-(Ethane-1,2-diyl) Bis(2-bromoethanamide) (3a).** FT-IR (Solid): 3294  $\text{cm}^{-1}$  (amide N–H str.), 2938  $\text{cm}^{-1}$  ( $-\text{CH}_2-$  assym. str.), 2860  $\text{cm}^{-1}$  ( $-\text{CH}_2-$  sym. str.), 1645  $\text{cm}^{-1}$  (Amide I,  $\text{C}=\text{O}$  str.), 1542  $\text{cm}^{-1}$  (Amide II, N–H ben.), 1480  $\text{cm}^{-1}$  ( $-\text{CH}_2-$  scissor).  $^1\text{H}$  NMR (400 MHz,  $\text{CDCl}_3$ ):  $\delta$  3.290 (m,  $-\text{NH}(\text{CH}_2)_2\text{NH}-$ , 4H), 3.873 (s,  $-\text{CH}_2\text{CONH}(\text{CH}_2)_2\text{NHCOC}_2-$ , 4H), 6.551 (br s, amide  $-\text{CONH}(\text{CH}_2)_2\text{NHCO}-$ , 2H).  $^{13}\text{C}$  NMR (100 MHz,  $\text{CDCl}_3$ ):  $\delta$  29.495, 40.134, 165.531.

**N,N'-(Propane-1,3-diyl) Bis(2-bromoethanamide) (3b).** FT-IR (Solid): 3295  $\text{cm}^{-1}$  (amide N–H str.), 2942  $\text{cm}^{-1}$  ( $-\text{CH}_2-$  assym. str.), 2863  $\text{cm}^{-1}$  ( $-\text{CH}_2-$  sym. str.), 1645  $\text{cm}^{-1}$  (Amide I,  $\text{C}=\text{O}$  str.), 1544  $\text{cm}^{-1}$  (Amide II, N–H ben.), 1485  $\text{cm}^{-1}$  ( $-\text{CH}_2-$  scissor).  $^1\text{H}$  NMR (400 MHz,  $\text{CDCl}_3$ ):  $\delta$  1.542 (m,  $-\text{CH}_2\text{CH}_2\text{CH}_2-$ , 4H), 3.291 (m,  $-\text{NHCH}_2\text{CH}_2\text{CH}_2\text{NH}-$ , 4H), 3.876 (s,  $-\text{CH}_2\text{CONH}(\text{CH}_2)_3\text{NHCOC}_2-$ , 4H), 6.589 (br s, amide  $-\text{CONH}(\text{CH}_2)_3\text{NHCO}-$ , 2H).  $^{13}\text{C}$  NMR (100 MHz,  $\text{CDCl}_3$ ):  $\delta$  29.239, 29.482, 40.194, 165.538.

**N,N'-(Butane-1,4-diyl) Bis(2-bromoethanamide) (3c).** FT-IR (Solid): 3294  $\text{cm}^{-1}$  (amide N–H str.), 2939  $\text{cm}^{-1}$  ( $-\text{CH}_2-$  assym. str.), 2859  $\text{cm}^{-1}$  ( $-\text{CH}_2-$  sym. str.), 1642  $\text{cm}^{-1}$  (Amide I,  $\text{C}=\text{O}$  str.), 1545  $\text{cm}^{-1}$  (Amide II, N–H ben.), 1480  $\text{cm}^{-1}$  ( $-\text{CH}_2-$  scissor).  $^1\text{H}$  NMR (400 MHz,  $\text{CDCl}_3$ ):  $\delta$  1.541 (m,  $-\text{CH}_2(\text{CH}_2)_2\text{CH}_2-$ , 4H), 3.293 (q,  $-\text{CH}_2(\text{CH}_2)_2\text{CH}_2-$ , 4H), 3.874 (s,  $-\text{CH}_2\text{CONH}(\text{CH}_2)_4\text{NHCOC}_2-$ , 4H), 6.554 (br s, amide  $-\text{CONH}(\text{CH}_2)_4\text{NHCO}-$ , 2H).  $^{13}\text{C}$  NMR (100 MHz,  $\text{CDCl}_3$ ):  $\delta$  29.254, 29.479, 40.294, 165.540.

**N,N'-(Hexane-1,6-diyl) Bis(2-bromoethanamide) (3d).** ATR FT-IR (Solid): 3295  $\text{cm}^{-1}$  (amide N–H str.), 2937  $\text{cm}^{-1}$  ( $-\text{CH}_2-$  assym. str.), 2858  $\text{cm}^{-1}$  ( $-\text{CH}_2-$  sym. str.), 1639  $\text{cm}^{-1}$  (Amide I,  $\text{C}=\text{O}$  str.), 1540  $\text{cm}^{-1}$  (Amide II, N–H ben.), 1483  $\text{cm}^{-1}$  ( $-\text{CH}_2-$  scissor).  $^1\text{H}$  NMR (400 MHz,  $\text{CDCl}_3$ ):  $\delta$  1.369 (m,  $-\text{CH}_2\text{CH}_2(\text{CH}_2)_2\text{CH}_2\text{CH}_2-$ , 4H), 1.539 (m,  $-\text{CH}_2\text{CH}_2(\text{CH}_2)_2\text{CH}_2\text{CH}_2-$ , 4H), 3.293 (q,  $-\text{CH}_2\text{CH}_2(\text{CH}_2)_2\text{CH}_2\text{CH}_2-$ , 4H), 3.877 (s,  $-\text{CH}_2\text{CONH}(\text{CH}_2)_6\text{NHCOC}_2-$ , 4H), 6.548 (br s, amide  $-\text{CONH}(\text{CH}_2)_6\text{NHCO}-$ , 2H).  $^{13}\text{C}$  NMR (100 MHz,  $\text{CDCl}_3$ ):  $\delta$  26.268, 29.264, 29.485, 40.034, 165.531.

**General Procedure for the Synthesis of Cationic Small Molecules (4–19).** To the individual solutions of 3a–3d (4 mmol) in organic solvents (EtOH for 3a,  $\text{CHCl}_3$  for 3b, and MeCN for 3c and 3d, 50 mL) were added 2a–2d (12 mmol) separately, and the reaction mixtures were stirred at 85 °C for about 24 h. After the reaction, the mixtures were cooled to room temperature and transferred to a RB flask. Then the volume of the reaction mixtures was reduced to 1/10th its original volume by rotary evaporator. Finally, the products were precipitated with excess diethyl ether/acetone (150 mL). Either the organic solvent was decanted off and the precipitate was washed three times with diethyl ether, or the precipitates were filtered through sintered glass funnel and washed repeatedly with diethyl ether and vacuum-dried to give more than 99% yield. All the final products (4–19) were characterized by FT-IR,  $^1\text{H}$  NMR,  $^{13}\text{C}$  NMR, HRMS, and elemental analysis. The purity of the compounds checked by reverse phase high performance liquid chromatography (HPLC) using 0.1% trifluoroacetic acid (TFA) in water/acetonitrile (0–100%) as mobile phase was more than 95%.

**N,N'-(Ethane-1,2-diethanamide) Bis(N,N-dimethyl-(N'-hexylethanamide) ammonium bromide) (4).** FTIR (Solid): 3208  $\text{cm}^{-1}$  (amide N–H str.), 2909  $\text{cm}^{-1}$  ( $-\text{CH}_2-$  assym. str.), 2860  $\text{cm}^{-1}$  ( $-\text{CH}_2-$  sym. str.), 1675  $\text{cm}^{-1}$  (amide I,  $\text{C}=\text{O}$  str.), 1555  $\text{cm}^{-1}$  (amide II, N–H ben.), 1468  $\text{cm}^{-1}$  ( $-\text{CH}_2-$  scissor).  $^1\text{H}$  NMR (400 MHz,  $\text{CDCl}_3$ ):  $\delta$  0.875 (t, terminal  $-\text{CH}_3$ , 6H), 1.259 (m,  $-\text{CH}_3(\text{CH}_2)_3\text{CH}_2-$ , 12H), 1.581 (m,  $\text{CH}_3(\text{CH}_2)_3\text{CH}_2\text{CH}_2-$ , 4H), 3.231 (m,  $\text{CH}_3(\text{CH}_2)_3\text{CH}_2\text{CH}_2-$ , 4H), 3.439 (m,  $-\text{NHCH}_2\text{CH}_2\text{NH}-$ , 4H), 3.611 (s,  $-\text{CH}_2\text{N}^+(\text{CH}_3)_2\text{CH}_2-$ , 12H), 4.630 (s,  $-\text{CH}_2\text{N}^+(\text{CH}_3)_2\text{CH}_2-$ , 4H), 8.219 (br s,  $\text{CH}_3(\text{CH}_2)_5\text{NHCO}-$ , 2H), 8.684 (br s,  $-\text{CONHCH}_2-$ , 2H).  $^{13}\text{C}$  NMR (100 MHz,  $\text{CDCl}_3$ ):  $\delta$  14.219, 22.777, 27.281, 29.225, 29.415, 38.941, 40.409, 52.829, 64.182, 66.226, 162.664, 162.880. HRMS (ESI)  $m/z$  calculated for  $\text{C}_{26}\text{H}_{54}\text{N}_6\text{O}_4\text{Br}_2$  [M – Br] $^+$  and [M – 2Br] $^{2+}$ : 593.3571, 595.3571, and 257.2112. Found: 593.3394, 595.3379, and 257.2112.

**N,N'-(Propane-1,3-diethanamide) Bis(N,N-dimethyl-(N'-hexylethanamide) ammonium bromide) (5).** FTIR (Solid): 3212  $\text{cm}^{-1}$  (amide N–H str.), 2928  $\text{cm}^{-1}$  ( $-\text{CH}_2-$  assym. str.), 2860  $\text{cm}^{-1}$  ( $-\text{CH}_2-$  sym. str.), 1685  $\text{cm}^{-1}$  (amide I,  $\text{C}=\text{O}$  str.), 1565  $\text{cm}^{-1}$  (amide II, N–H ben.), 1465  $\text{cm}^{-1}$  ( $-\text{CH}_2-$  scissor).  $^1\text{H}$  NMR (400 MHz,  $\text{CDCl}_3$ ):  $\delta$  0.862 (t, terminal  $-\text{CH}_3$ , 6H), 1.269 (m,  $-\text{CH}_3(\text{CH}_2)_3\text{CH}_2-$ , 12H), 1.615 (m,  $\text{CH}_3(\text{CH}_2)_3\text{CH}_2\text{CH}_2-$ , 4H), 1.851 (m,  $-\text{NHCH}_2\text{CH}_2\text{CH}_2\text{NH}-$ , 2H), 3.231 (m,  $\text{CH}_3(\text{CH}_2)_3\text{CH}_2\text{CH}_2-$ , 4H), 3.381 (m,  $-\text{NHCH}_2\text{CH}_2\text{CH}_2\text{NH}-$ , 4H), 3.580 (s,  $-\text{CH}_2\text{N}^+(\text{CH}_3)_2\text{CH}_2-$ , 12H), 4.614 (s,  $-\text{CH}_2\text{N}^+(\text{CH}_3)_2\text{CH}_2-$ , 4H), 8.208 (br s,  $\text{CH}_3(\text{CH}_2)_5\text{NHCO}-$ , 2H), 8.665 (br s,  $-\text{CONHCH}_2-$ , 2H).  $^{13}\text{C}$  NMR (100 MHz,  $\text{CDCl}_3$ ):  $\delta$  14.209, 22.707, 26.138, 27.278, 29.224, 29.409, 38.978, 40.412, 52.838, 64.194, 66.234, 162.647, 162.856. HRMS (ESI)  $m/z$  calculated for  $\text{C}_{27}\text{H}_{56}\text{N}_6\text{O}_4\text{Br}_2$  [M – Br] $^+$  and [M – 2Br] $^{2+}$ : 607.3726, 609.3726, and 264.2272. Found: 607.2185, 609.3509, and 264.2185.

**N,N'-(Butane-1,4-diethanamide) Bis(N,N-dimethyl-(N'-hexylethanamide) ammonium bromide) (6).** FTIR (Solid): 3210  $\text{cm}^{-1}$  (amide N–H str.), 2920  $\text{cm}^{-1}$  ( $-\text{CH}_2-$  assym. str.), 2860  $\text{cm}^{-1}$  ( $-\text{CH}_2-$  sym. str.), 1678  $\text{cm}^{-1}$  (amide I,  $\text{C}=\text{O}$  str.), 1557  $\text{cm}^{-1}$  (amide II, N–H ben.), 1470  $\text{cm}^{-1}$  ( $-\text{CH}_2-$  scissor).  $^1\text{H}$  NMR (400 MHz,  $\text{CDCl}_3$ ):  $\delta$  0.872 (t, terminal  $-\text{CH}_3$ , 6H), 1.254 (m,  $-\text{CH}_3(\text{CH}_2)_3\text{CH}_2-$ , 12H), 1.534 (m,  $\text{CH}_3(\text{CH}_2)_3\text{CH}_2\text{CH}_2-$ , 4H), 1.578 (m,  $-\text{NHCH}_2(\text{CH}_2)_2\text{CH}_2\text{NH}-$ , 4H), 3.220 (m,  $\text{CH}_3(\text{CH}_2)_3\text{CH}_2\text{CH}_2-$ , 4H), 3.321 (m,  $-\text{NHCH}_2(\text{CH}_2)_2\text{CH}_2\text{NH}-$ , 4H), 3.558 (s,  $-\text{CH}_2\text{N}^+(\text{CH}_3)_2\text{CH}_2-$ , 12H), 4.610 (s,  $-\text{CH}_2\text{N}^+(\text{CH}_3)_2\text{CH}_2-$ , 4H), 8.205 (br s,  $\text{CH}_3(\text{CH}_2)_7\text{NHCO}-$ , 2H),

8.447 (br s,  $-\text{CONHCH}_2-$ , 2H).  $^{13}\text{C}$  NMR (100 MHz,  $\text{CDCl}_3$ ):  $\delta$  14.221, 22.760, 26.108, 27.144, 27.173, 29.308, 29.336, 31.160, 40.056, 52.788, 64.447, 65.532, 162.773, 162.943. HRMS (ESI)  $m/z$  calculated for  $\text{C}_{28}\text{H}_{58}\text{N}_6\text{O}_4\text{Br}_2$  [ $\text{M} - \text{Br}]^+$  and  $[\text{M} - 2\text{Br}]^{2+}$ : 677.4510, 679.4510, and 299.2663. Found: 677.4306, 679.4290, and 299.2618.

*N,N'-(Hexane-1,6-diethanamide) Bis(N,N-dimethyl-(N'-hexylethanamide) ammonium bromide) (7).* FTIR (Solid): 3207  $\text{cm}^{-1}$  (amide N–H str.), 2914  $\text{cm}^{-1}$  ( $-\text{CH}_2-$  assym. str.), 2855  $\text{cm}^{-1}$  ( $-\text{CH}_2-$  sym. str.), 1675  $\text{cm}^{-1}$  (amide I, C=O str.), 1558  $\text{cm}^{-1}$  (amide II, N–H ben.), 1470  $\text{cm}^{-1}$  ( $-\text{CH}_2-$  scissor).  $^1\text{H}$  NMR (400 MHz,  $\text{CDCl}_3$ ):  $\delta$  0.875 (t, terminal  $-\text{CH}_3$ , 6H), 1.262 (m,  $-\text{CH}_3(\text{CH}_2)_5\text{CH}_2-$ , 20H), 1.414 (m,  $-\text{NHCH}_2\text{CH}_2(\text{CH}_2)_2\text{CH}_2\text{CH}_2\text{NH}-$ , 4H), 1.554–1.571 (m,  $-\text{CH}_3(\text{CH}_2)_5\text{CH}_2\text{CH}_2-$  and  $-\text{NHCH}_2\text{CH}_2(\text{CH}_2)_2\text{CH}_2\text{CH}_2\text{NH}-$ , 8H), 3.241–3.316 (m,  $\text{CH}_3(\text{CH}_2)_5\text{CH}_2\text{CH}_2-$  and  $-\text{NHCH}_2(\text{CH}_2)_4\text{CH}_2\text{NH}-$ , 8H), 3.586 (s,  $-\text{CH}_2\text{N}^+(\text{CH}_3)_2\text{CH}_2-$ , 12H), 4.641 (s,  $-\text{CH}_2\text{N}^+(\text{CH}_3)_2\text{CH}_2-$ , 4H), 8.229 (br s,  $\text{CH}_3(\text{CH}_2)_7\text{NHCO}-$ , 2H), 8.440 (br s,  $-\text{CONHCH}_2-$ , 2H).  $^{13}\text{C}$  NMR (100 MHz,  $\text{CDCl}_3$ ):  $\delta$  14.206, 22.743, 26.198, 27.129, 28.308, 29.156, 29.297, 29.320, 39.313, 40.040, 52.621, 64.782, 65.243, 162.765, 162.862. HRMS (ESI)  $m/z$  calculated for  $\text{C}_{30}\text{H}_{62}\text{N}_6\text{O}_4\text{Br}_2$  [ $\text{M} - \text{Br}]^+$  and  $[\text{M} - 2\text{Br}]^{2+}$ : 649.4197, 651.4197, and 285.2507. Found: 649.4109, 651.4098, and 285.2493.

*N,N'-(Ethane-1,2-diethanamide) Bis(N,N-dimethyl-(N'-octylethanamide) ammonium bromide) (8).* FTIR (Solid): 3215  $\text{cm}^{-1}$  (amide N–H str.), 2918  $\text{cm}^{-1}$  ( $-\text{CH}_2-$  assym. str.), 2855  $\text{cm}^{-1}$  ( $-\text{CH}_2-$  sym. str.), 1678  $\text{cm}^{-1}$  (amide I, C=O str.), 1560  $\text{cm}^{-1}$  (amide II, N–H ben.), 1465  $\text{cm}^{-1}$  ( $-\text{CH}_2-$  scissor).  $^1\text{H}$  NMR (400 MHz,  $\text{CDCl}_3$ ):  $\delta$  0.866 (t, terminal  $-\text{CH}_3$ , 6H), 1.266 (m,  $-\text{CH}_3(\text{CH}_2)_5\text{CH}_2-$ , 20H), 1.564 (m,  $\text{CH}_3(\text{CH}_2)_5\text{CH}_2\text{CH}_2-$ , 4H), 3.229 (m,  $\text{CH}_3(\text{CH}_2)_5\text{CH}_2\text{CH}_2-$ , 4H), 3.459 (m,  $-\text{NHCH}_2\text{CH}_2\text{NH}-$ , 4H), 3.605 (s,  $-\text{CH}_2\text{N}^+(\text{CH}_3)_2\text{CH}_2-$ , 12H), 4.629 (s,  $-\text{CH}_2\text{N}^+(\text{CH}_3)_2\text{CH}_2-$ , 4H), 8.234 (br s,  $\text{CH}_3(\text{CH}_2)_7\text{NHCO}-$ , 2H), 8.734 (br s,  $-\text{CONHCH}_2-$ , 2H).  $^{13}\text{C}$  NMR (100 MHz,  $\text{CDCl}_3$ ):  $\delta$  14.228, 22.767, 27.163, 29.180, 29.313, 29.338, 31.939, 38.822, 40.403, 52.829, 64.122, 66.238, 162.765, 163.380. HRMS (ESI)  $m/z$  calculated for  $\text{C}_{30}\text{H}_{62}\text{N}_6\text{O}_4\text{Br}_2$  [ $\text{M} - \text{Br}]^+$  and  $[\text{M} - 2\text{Br}]^{2+}$ : 649.4197, 651.4197, and 285.2507. Found: 649.4109, 651.4098, and 285.2493. Elemental analysis: C 49.43, H 8.58, N 11.54 (calculated); C 49.23, H 8.60, N 11.29 (found).

*N,N'-(Propyl-1,3-diethanamide) Bis(N,N-dimethyl-(N'-octylethanamide) ammonium bromide) (9).* FTIR (Solid): 3210  $\text{cm}^{-1}$  (amide N–H str.), 2925  $\text{cm}^{-1}$  ( $-\text{CH}_2-$  assym. str.), 2860  $\text{cm}^{-1}$  ( $-\text{CH}_2-$  sym. str.), 1680  $\text{cm}^{-1}$  (amide I, C=O str.), 1565  $\text{cm}^{-1}$  (amide II, N–H ben.), 1470  $\text{cm}^{-1}$  ( $-\text{CH}_2-$  scissor).  $^1\text{H}$  NMR (400 MHz,  $\text{CDCl}_3$ ):  $\delta$  0.860 (t, terminal  $-\text{CH}_3$ , 6H), 1.264 (m,  $-\text{CH}_3(\text{CH}_2)_5\text{CH}_2-$ , 20H), 1.555 (m,  $\text{CH}_3(\text{CH}_2)_5\text{CH}_2\text{CH}_2-$ , 4H), 1.848 (m,  $-\text{NHCH}_2\text{CH}_2\text{CH}_2\text{NH}-$ , 2H), 3.241 (m,  $\text{CH}_3(\text{CH}_2)_5\text{CH}_2\text{CH}_2-$ , 4H), 3.377 (m,  $-\text{NHCH}_2\text{CH}_2\text{CH}_2\text{NH}-$ , 4H), 3.583 (s,  $-\text{CH}_2\text{N}^+(\text{CH}_3)_2\text{CH}_2-$ , 12H), 4.666 (s,  $-\text{CH}_2\text{N}^+(\text{CH}_3)_2\text{CH}_2-$ , 4H), 8.178 (br s,  $\text{CH}_3(\text{CH}_2)_7\text{NHCO}-$ , 2H), 8.601 (br s,  $-\text{CONHCH}_2-$ , 2H).  $^{13}\text{C}$  NMR (100 MHz,  $\text{CDCl}_3$ ):  $\delta$  14.201, 22.790, 26.128, 27.134, 27.189, 29.412, 29.289, 31.260, 40.456, 52.898, 64.401, 65.516, 162.768, 162.848. HRMS (ESI)  $m/z$  calculated for  $\text{C}_{31}\text{H}_{64}\text{N}_6\text{O}_4\text{Br}_2$  [ $\text{M} - \text{Br}]^+$  and  $[\text{M} - 2\text{Br}]^{2+}$ : 663.4354, 665.4354, and 292.2585. Found: 663.4164, 665.4133, and 292.2564. Elemental analysis: C 50.11, H 8.69, N 11.32 (calculated); C 50.01, H 8.60, N 11.24 (found).

*N,N'-(Butane-1,4-diethanamide) Bis(N,N-dimethyl-(N'-octylethanamide) ammonium bromide) (10).* FTIR (Solid): 3205  $\text{cm}^{-1}$  (amide N–H str.), 2915  $\text{cm}^{-1}$  ( $-\text{CH}_2-$  assym. str.), 2852  $\text{cm}^{-1}$  ( $-\text{CH}_2-$  sym. str.), 1674  $\text{cm}^{-1}$  (amide I, C=O str.), 1560  $\text{cm}^{-1}$  (amide II, N–H ben.), 1468  $\text{cm}^{-1}$  ( $-\text{CH}_2-$  scissor).  $^1\text{H}$  NMR (400 MHz,  $\text{CDCl}_3$ ):  $\delta$  0.864 (t, terminal  $-\text{CH}_3$ , 6H), 1.262 (m,  $-\text{CH}_3(\text{CH}_2)_5\text{CH}_2-$ , 20H), 1.544 (m,  $\text{CH}_3(\text{CH}_2)_5\text{CH}_2\text{CH}_2-$ , 4H), 1.580 (m,  $-\text{NHCH}_2(\text{CH}_2)_2\text{CH}_2\text{NH}-$ , 4H), 3.213 (m,  $\text{CH}_3(\text{CH}_2)_5\text{CH}_2\text{CH}_2-$ , 4H), 3.316 (m,  $-\text{NHCH}_2(\text{CH}_2)_2\text{CH}_2\text{NH}-$ , 4H), 3.558 (s,  $-\text{CH}_2\text{N}^+(\text{CH}_3)_2\text{CH}_2-$ , 12H), 4.610 (s,  $-\text{CH}_2\text{N}^+(\text{CH}_3)_2\text{CH}_2-$ , 4H), 8.205 (br s,  $\text{CH}_3(\text{CH}_2)_7\text{NHCO}-$ , 2H), 8.447 (br s,  $-\text{CONHCH}_2-$ , 2H).  $^{13}\text{C}$  NMR (100 MHz,  $\text{CDCl}_3$ ):  $\delta$

14.221, 22.760, 26.108, 27.144, 27.173, 29.308, 29.336, 31.160, 40.056, 52.788, 64.447, 65.532, 162.773, 162.943. HRMS (ESI)  $m/z$  calculated for  $\text{C}_{32}\text{H}_{66}\text{N}_6\text{O}_4\text{Br}_2$  [ $\text{M} - \text{Br}]^+$  and  $[\text{M} - 2\text{Br}]^{2+}$ : 677.4510, 679.4510, and 299.2663. Found: 677.4306, 679.4290, and 299.2618. Elemental analysis: C 50.76, H 8.79, N 11.11 (calculated); C 50.64, H 8.77, N 11.06 (found).

*N,N'-(Hexane-1,6-diethanamide) Bis(N,N-dimethyl-(N'-octylethanamide) ammonium bromide) (11).* FTIR (Solid): 3207  $\text{cm}^{-1}$  (amide N–H str.), 2914  $\text{cm}^{-1}$  ( $-\text{CH}_2-$  assym. str.), 2855  $\text{cm}^{-1}$  ( $-\text{CH}_2-$  sym. str.), 1675  $\text{cm}^{-1}$  (amide I, C=O str.), 1558  $\text{cm}^{-1}$  (amide II, N–H ben.), 1470  $\text{cm}^{-1}$  ( $-\text{CH}_2-$  scissor).  $^1\text{H}$  NMR (400 MHz,  $\text{CDCl}_3$ ):  $\delta$  0.875 (t, terminal  $-\text{CH}_3$ , 6H), 1.262 (m,  $-\text{CH}_3(\text{CH}_2)_5\text{CH}_2-$ , 20H), 1.414 (m,  $-\text{NHCH}_2\text{CH}_2(\text{CH}_2)_2\text{CH}_2\text{CH}_2\text{NH}-$ , 4H), 1.554–1.571 (m,  $-\text{CH}_3(\text{CH}_2)_5\text{CH}_2\text{CH}_2-$  and  $-\text{NHCH}_2\text{CH}_2(\text{CH}_2)_2\text{CH}_2\text{CH}_2\text{NH}-$ , 8H), 3.241–3.316 (m,  $\text{CH}_3(\text{CH}_2)_5\text{CH}_2\text{CH}_2-$  and  $-\text{NHCH}_2(\text{CH}_2)_4\text{CH}_2\text{NH}-$ , 8H), 3.586 (s,  $-\text{CH}_2\text{N}^+(\text{CH}_3)_2\text{CH}_2-$ , 12H), 4.641 (s,  $-\text{CH}_2\text{N}^+(\text{CH}_3)_2\text{CH}_2-$ , 4H), 8.229 (br s,  $\text{CH}_3(\text{CH}_2)_7\text{NHCO}-$ , 2H), 8.440 (br s,  $-\text{CONHCH}_2-$ , 2H).  $^{13}\text{C}$  NMR (100 MHz,  $\text{CDCl}_3$ ):  $\delta$  14.206, 22.743, 26.198, 27.129, 28.308, 29.156, 29.297, 29.320, 39.313, 40.040, 52.621, 64.782, 65.243, 162.765, 162.862. HRMS (ESI)  $m/z$  calculated for  $\text{C}_{34}\text{H}_{70}\text{N}_6\text{O}_4\text{Br}_2$  [ $\text{M} - \text{Br}]^+$  and  $[\text{M} - 2\text{Br}]^{2+}$ : 705.4824, 707.4824, and 313.2820. Found: 705.4618, 707.4602, and 313.2761. Elemental analysis: C 52.01, H 8.99, N 10.71 (calculated); C 51.95, H 8.84, N 10.36 (found).

*N,N'-(Ethane-1,2-diethanamide) Bis(N,N-dimethyl-(N'-dodecylethanamide) ammonium bromide) (12).* FTIR (Solid): 3212  $\text{cm}^{-1}$  (amide N–H str.), 2920  $\text{cm}^{-1}$  ( $-\text{CH}_2-$  assym. str.), 2860  $\text{cm}^{-1}$  ( $-\text{CH}_2-$  sym. str.), 1682  $\text{cm}^{-1}$  (amide I, C=O str.), 1565  $\text{cm}^{-1}$  (amide II, N–H ben.), 1468  $\text{cm}^{-1}$  ( $-\text{CH}_2-$  scissor).  $^1\text{H}$  NMR (400 MHz,  $\text{CDCl}_3$ ):  $\delta$  0.886 (t, terminal  $-\text{CH}_3$ , 6H), 1.259 (m,  $-\text{CH}_3(\text{CH}_2)_9\text{CH}_2-$ , 36H), 1.589 (m,  $\text{CH}_3(\text{CH}_2)_9\text{CH}_2\text{CH}_2-$ , 4H), 3.219 (m,  $\text{CH}_3(\text{CH}_2)_9\text{CH}_2\text{CH}_2-$ , 4H), 3.459 (m,  $-\text{NHCH}_2\text{CH}_2\text{NH}-$ , 4H), 3.612 (s,  $-\text{CH}_2\text{N}^+(\text{CH}_3)_2\text{CH}_2-$ , 12H), 4.627 (s,  $-\text{CH}_2\text{N}^+(\text{CH}_3)_2\text{CH}_2-$ , 4H), 8.229 (br s,  $\text{CH}_3(\text{CH}_2)_{11}\text{NHCO}-$ , 2H), 8.824 (br s,  $-\text{CONHCH}_2-$ , 2H).  $^{13}\text{C}$  NMR (100 MHz,  $\text{CDCl}_3$ ):  $\delta$  14.198, 22.801, 27.098, 29.280, 29.320, 29.431, 29.718, 32.401, 38.816, 40.415, 52.909, 64.221, 66.285, 162.749, 163.258. HRMS (ESI)  $m/z$  calculated for  $\text{C}_{38}\text{H}_{78}\text{N}_6\text{O}_4\text{Br}_2$  [ $\text{M} - \text{Br}]^+$  and  $[\text{M} - 2\text{Br}]^{2+}$ : 761.5450, 763.5450, and 341.3133. Found: 761.5241, 763.5229, and 341.3037. Elemental analysis: C 54.26, H 9.35, N 9.99 (calculated); C 54.16, H 9.41, N 9.91 (found).

*N,N'-(Propene-1,3-diethanamide) Bis(N,N-dimethyl-(N'-dodecylethanamide) ammonium bromide) (13).* FTIR (Solid): 3214  $\text{cm}^{-1}$  (amide N–H str.), 2929  $\text{cm}^{-1}$  ( $-\text{CH}_2-$  assym. str.), 2862  $\text{cm}^{-1}$  ( $-\text{CH}_2-$  sym. str.), 1681  $\text{cm}^{-1}$  (amide I, C=O str.), 1562  $\text{cm}^{-1}$  (amide II, N–H ben.), 1468  $\text{cm}^{-1}$  ( $-\text{CH}_2-$  scissor).  $^1\text{H}$  NMR (400 MHz,  $\text{CDCl}_3$ ):  $\delta$  0.877 (t, terminal  $-\text{CH}_3$ , 6H), 1.264 (m,  $-\text{CH}_3(\text{CH}_2)_9\text{CH}_2-$ , 36H), 1.521 (m,  $\text{CH}_3(\text{CH}_2)_9\text{CH}_2\text{CH}_2-$ , 4H), 1.839 (m,  $-\text{NHCH}_2\text{CH}_2\text{CH}_2\text{NH}-$ , 2H), 3.250 (m,  $\text{CH}_3(\text{CH}_2)_9\text{CH}_2\text{CH}_2-$ , 4H), 3.379 (m,  $-\text{NHCH}_2\text{CH}_2\text{CH}_2\text{NH}-$ , 4H), 3.579 (s,  $-\text{CH}_2\text{N}^+(\text{CH}_3)_2\text{CH}_2-$ , 12H), 4.689 (s,  $-\text{CH}_2\text{N}^+(\text{CH}_3)_2\text{CH}_2-$ , 4H), 8.210 (br s,  $\text{CH}_3(\text{CH}_2)_{11}\text{NHCO}-$ , 2H), 8.612 (br s,  $-\text{CONHCH}_2-$ , 2H).  $^{13}\text{C}$  NMR (100 MHz,  $\text{CDCl}_3$ ):  $\delta$  14.218, 22.789, 27.112, 29.310, 29.318, 29.428, 29.595, 29.710, 32.412, 38.821, 40.421, 52.913, 64.230, 66.290, 162.752, 163.308. HRMS (ESI)  $m/z$  calculated for  $\text{C}_{39}\text{H}_{80}\text{N}_6\text{O}_4\text{Br}_2$  [ $\text{M} - \text{Br}]^+$  and  $[\text{M} - 2\text{Br}]^{2+}$ : 775.1874, 777.1874, and 348.1345. Found: 775.1396, 777.1381, and 348.1123. Elemental analysis: C 54.79, H 9.43, N 9.90 (calculated); C 54.72, H 9.51, N 9.86 (found).

*N,N'-(Butane-1,4-diethanamide) Bis(N,N-dimethyl-(N'-dodecylethanamide) ammonium bromide) (14).* FTIR (Solid): 3210  $\text{cm}^{-1}$  (amide N–H str.), 2912  $\text{cm}^{-1}$  ( $-\text{CH}_2-$  assym. str.), 2855  $\text{cm}^{-1}$  ( $-\text{CH}_2-$  sym. str.), 1675  $\text{cm}^{-1}$  (amide I, C=O str.), 1563  $\text{cm}^{-1}$  (amide II, N–H ben.), 1470  $\text{cm}^{-1}$  ( $-\text{CH}_2-$  scissor).  $^1\text{H}$  NMR (400 MHz,  $\text{CDCl}_3$ ):  $\delta$  0.878 (t, terminal  $-\text{CH}_3$ , 6H), 1.257 (m,  $-\text{CH}_3(\text{CH}_2)_9\text{CH}_2-$ , 36H), 1.539 (m,  $\text{CH}_3(\text{CH}_2)_9\text{CH}_2\text{CH}_2-$ , 4H), 1.578 (m,  $-\text{NHCH}_2(\text{CH}_2)_2\text{CH}_2\text{NH}-$ , 4H), 3.218 (m,  $\text{CH}_3(\text{CH}_2)_9\text{CH}_2\text{CH}_2-$ , 4H), 3.320 (m,  $-\text{NHCH}_2(\text{CH}_2)_2\text{CH}_2\text{NH}-$ ,

4H), 3.560 (s,  $-\text{CH}_2\text{N}^+(\text{CH}_3)_2\text{CH}_2-$ , 12H), 4.612 (s,  $-\text{CH}_2\text{N}^+(\text{CH}_3)_2\text{CH}_2-$ , 4H), 8.218 (br s,  $\text{CH}_3(\text{CH}_2)_{11}\text{NHCO}-$ , 2H), 8.451 (br s,  $-\text{CONHCH}_2-$ , 2H).  $^{13}\text{C}$  NMR (100 MHz,  $\text{CDCl}_3$ ):  $\delta$  14.220, 22.791, 27.110, 29.312, 29.321, 29.425, 29.598, 29.707, 32.417, 38.821, 40.418, 52.924, 64.232, 66.288, 162.756, 163.310. HRMS (ESI)  $m/z$  calculated for  $\text{C}_{40}\text{H}_{82}\text{N}_6\text{O}_4\text{Br}_2$  [M - Br]<sup>+</sup> and [M - 2Br]<sup>2+</sup>: 789.763, 791.5763, and 355.329. Found: 789.5557, 791.5545, and 355.3197. Elemental analysis: C 55.29, H 9.52, N 9.67 (calculated); C 55.25, H 9.49, N 9.62 (found).

*N,N'-(Hexane-1,6-diethanamide) Bis(N,N-dimethyl-(N'-dodecylethanamide) ammonium bromide) (15).* FTIR (Solid): 3210  $\text{cm}^{-1}$  (amide N-H str.), 2918  $\text{cm}^{-1}$  ( $-\text{CH}_2-$  assym. str.), 2858  $\text{cm}^{-1}$  ( $-\text{CH}_2-$  sym. str.), 1676  $\text{cm}^{-1}$  (amide I, C=O str.), 1560  $\text{cm}^{-1}$  (amide II, N-H ben.), 1465  $\text{cm}^{-1}$  ( $-\text{CH}_2-$  scissor).  $^1\text{H}$  NMR (400 MHz,  $\text{CDCl}_3$ ):  $\delta$  0.879 (t, terminal  $-\text{CH}_3$ , 6H), 1.258 (m,  $-\text{CH}_3(\text{CH}_2)_9\text{CH}_2-$ , 36H), 1.421 (m,  $-\text{NHCH}_2\text{CH}_2(\text{CH}_2)_2\text{CH}_2\text{CH}_2\text{NH}-$ , 4H), 1.552–1.574 (m,  $-\text{CH}_3(\text{CH}_2)_9\text{CH}_2\text{CH}_2-$  and  $-\text{NHCH}_2\text{CH}_2(\text{CH}_2)_2\text{CH}_2\text{CH}_2\text{NH}-$ , 8H), 3.240–3.318 (m,  $\text{CH}_3(\text{CH}_2)_9\text{CH}_2\text{CH}_2-$  and  $-\text{NHCH}_2(\text{CH}_2)_4\text{CH}_2\text{NH}-$ , 8H), 3.588 (s,  $-\text{CH}_2\text{N}^+(\text{CH}_3)_2\text{CH}_2-$ , 12H), 4.642 (s,  $-\text{CH}_2\text{N}^+(\text{CH}_3)_2\text{CH}_2-$ , 4H), 8.227 (br s,  $\text{CH}_3(\text{CH}_2)_{11}\text{NHCO}-$ , 2H), 8.438 (br s,  $-\text{CONHCH}_2-$ , 2H).  $^{13}\text{C}$  NMR (100 MHz,  $\text{CDCl}_3$ ):  $\delta$  14.218, 22.786, 27.108, 29.318, 29.341, 29.435, 29.599, 29.714, 32.423, 38.828, 40.419, 52.928, 64.241, 66.294, 162.757, 163.312. HRMS (ESI)  $m/z$  calculated for  $\text{C}_{42}\text{H}_{86}\text{N}_6\text{O}_4\text{Br}_2$  [M - Br]<sup>+</sup> and [M - 2Br]<sup>2+</sup>: 817.6076, 819.6076, and 369.3446. Found: 817.5849, 819.5837, and 369.3339. Elemental analysis: C 56.22, H 9.67, N 9.37 (calculated); C 56.20, H 9.69, N 9.29 (found).

*N,N'-(Ethane-1,2-diethanamide) Bis(N,N-dimethyl-(N'-hexadecylethanamide) ammonium bromide) (16).* FTIR (Solid): 3208  $\text{cm}^{-1}$  (amide N-H str.), 2925  $\text{cm}^{-1}$  ( $-\text{CH}_2-$  assym. str.), 2862  $\text{cm}^{-1}$  ( $-\text{CH}_2-$  sym. str.), 1680  $\text{cm}^{-1}$  (amide I, C=O str.), 1560  $\text{cm}^{-1}$  (amide II, N-H ben.), 1467  $\text{cm}^{-1}$  ( $-\text{CH}_2-$  scissor).  $^1\text{H}$  NMR (400 MHz,  $\text{CDCl}_3$ ):  $\delta$  0.880 (t, terminal  $-\text{CH}_3$ , 6H), 1.249 (m,  $-\text{CH}_3(\text{CH}_2)_{13}\text{CH}_2-$ , 52H), 1.580 (m,  $\text{CH}_3(\text{CH}_2)_{13}\text{CH}_2\text{CH}_2-$ , 4H), 3.217 (m,  $\text{CH}_3(\text{CH}_2)_{13}\text{CH}_2\text{CH}_2-$ , 4H), 3.458 (m,  $-\text{NHCH}_2\text{CH}_2\text{NH}-$ , 4H), 3.618 (s,  $-\text{CH}_2\text{N}^+(\text{CH}_3)_2\text{CH}_2-$ , 12H), 4.628 (s,  $-\text{CH}_2\text{N}^+(\text{CH}_3)_2\text{CH}_2-$ , 4H), 8.224 (br s,  $\text{CH}_3(\text{CH}_2)_{15}\text{NHCO}-$ , 2H), 8.828 (br s,  $-\text{CONHCH}_2-$ , 2H).  $^{13}\text{C}$  NMR (100 MHz,  $\text{CDCl}_3$ ):  $\delta$  14.212, 22.745, 27.112, 29.321, 29.347, 29.429, 29.578, 29.726, 32.420, 38.824, 40.422, 52.931, 64.244, 66.289, 162.754, 163.307. HRMS (ESI)  $m/z$  calculated for  $\text{C}_{46}\text{H}_{94}\text{N}_6\text{O}_4\text{Br}_2$  [M - Br]<sup>+</sup> and [M - 2Br]<sup>2+</sup>: 873.6703, 875.6703, and 397.6760. Found: 873.6499, 875.6489, and 397.3687. Elemental analysis: C 57.95, H 9.94, N 8.82 (calculated); C 57.89, H 9.98, N 8.78 (found).

*N,N'-(Propane-1,3-diethanamide) Bis(N,N-dimethyl-(N'-hexadecylethanamide) ammonium bromide) (17).* FTIR (Solid): 3215  $\text{cm}^{-1}$  (amide N-H str.), 2930  $\text{cm}^{-1}$  ( $-\text{CH}_2-$  assym. str.), 2860  $\text{cm}^{-1}$  ( $-\text{CH}_2-$  sym. str.), 1682  $\text{cm}^{-1}$  (amide I, C=O str.), 1565  $\text{cm}^{-1}$  (amide II, N-H ben.), 1465  $\text{cm}^{-1}$  ( $-\text{CH}_2-$  scissor).  $^1\text{H}$  NMR (400 MHz,  $\text{CDCl}_3$ ):  $\delta$  0.881 (t, terminal  $-\text{CH}_3$ , 6H), 1.260 (m,  $-\text{CH}_3(\text{CH}_2)_{13}\text{CH}_2-$ , 52H), 1.531 (m,  $\text{CH}_3(\text{CH}_2)_{13}\text{CH}_2\text{CH}_2-$ , 4H), 1.842 (m,  $-\text{NHCH}_2\text{CH}_2\text{CH}_2\text{NH}-$ , 2H), 3.252 (m,  $\text{CH}_3(\text{CH}_2)_{13}\text{CH}_2\text{CH}_2-$ , 4H), 3.368 (m,  $-\text{NHCH}_2\text{CH}_2\text{CH}_2\text{NH}-$ , 4H), 3.584 (s,  $-\text{CH}_2\text{N}^+(\text{CH}_3)_2\text{CH}_2-$ , 12H), 4.682 (s,  $-\text{CH}_2\text{N}^+(\text{CH}_3)_2\text{CH}_2-$ , 4H), 8.206 (br s,  $\text{CH}_3(\text{CH}_2)_{15}\text{NHCO}-$ , 2H), 8.624 (br s,  $-\text{CONHCH}_2-$ , 2H).  $^{13}\text{C}$  NMR (100 MHz,  $\text{CDCl}_3$ ):  $\delta$  14.220, 22.789, 23.878, 27.142, 29.321, 29.334, 29.438, 29.584, 29.714, 32.425, 38.829, 40.427, 52.920, 64.238, 66.297, 162.757, 163.314. HRMS (ESI)  $m/z$  calculated for  $\text{C}_{47}\text{H}_{96}\text{N}_6\text{O}_4\text{Br}_2$  [M - Br]<sup>+</sup> and [M - 2Br]<sup>2+</sup>: 887.6859, 889.6859, and 404.3838. Found: 887.6662, 889.6652, and 404.3786. Elemental analysis: C 58.35, H 10.01, N 8.69 (calculated); C 58.27, H 10.11, N 8.58 (found).

*N,N'-(Butane-1,4-diethanamide) Bis(N,N-dimethyl-(N'-hexadecylethanamide) ammonium bromide) (18).* FTIR (Solid): 3205  $\text{cm}^{-1}$  (amide N-H str.), 2910  $\text{cm}^{-1}$  ( $-\text{CH}_2-$  assym. str.), 2850  $\text{cm}^{-1}$  ( $-\text{CH}_2-$  sym. str.), 1674  $\text{cm}^{-1}$  (amide I, C=O str.), 1560  $\text{cm}^{-1}$  (amide II, N-H ben.), 1464  $\text{cm}^{-1}$  ( $-\text{CH}_2-$  scissor).  $^1\text{H}$  NMR (400 MHz,  $\text{CDCl}_3$ ):  $\delta$  0.869 (t, terminal  $-\text{CH}_3$ , 6H), 1.251 (m,

$-\text{CH}_3(\text{CH}_2)_{13}\text{CH}_2-$ , 52H), 1.537 (m,  $\text{CH}_3(\text{CH}_2)_{13}\text{CH}_2\text{CH}_2-$ , 4H), 1.581 (m,  $-\text{NHCH}_2(\text{CH}_2)_2\text{CH}_2\text{NH}-$ , 4H), 3.220 (m,  $\text{CH}_3(\text{CH}_2)_{13}\text{CH}_2\text{CH}_2-$ , 4H), 3.324 (m,  $-\text{NHCH}_2(\text{CH}_2)_2\text{CH}_2\text{NH}-$ , 4H), 3.556 (s,  $-\text{CH}_2\text{N}^+(\text{CH}_3)_2\text{CH}_2-$ , 12H), 4.607 (s,  $-\text{CH}_2\text{N}^+(\text{CH}_3)_2\text{CH}_2-$ , 4H), 8.211 (br s,  $\text{CH}_3(\text{CH}_2)_{15}\text{NHCO}-$ , 2H), 8.454 (br s,  $-\text{CONHCH}_2-$ , 2H).  $^{13}\text{C}$  NMR (100 MHz,  $\text{CDCl}_3$ ):  $\delta$  14.217, 22.788, 23.867, 27.151, 29.318, 29.328, 29.441, 29.542, 29.708, 32.418, 38.820, 40.420, 52.918, 64.228, 66.290, 162.753, 163.322. HRMS (ESI)  $m/z$  calculated for  $\text{C}_{48}\text{H}_{98}\text{N}_6\text{O}_4\text{Br}_2$  [M - Br]<sup>+</sup> and [M - 2Br]<sup>2+</sup>: 901.7016, 903.7016, and 411.3916. Found: 901.6819, 903.6814, and 411.3865. Elemental analysis: C 58.74, H 10.07, N 8.57 (calculated); C 58.68, H 10.12, N 8.50 (found).

*N,N'-(Hexane-1,6-diethanamide) Bis(N,N-dimethyl-(N'-hexadecylethanamide) ammonium bromide) (19).* FTIR (Solid): 3208  $\text{cm}^{-1}$  (amide N-H str.), 2920  $\text{cm}^{-1}$  ( $-\text{CH}_2-$  assym. str.), 2860  $\text{cm}^{-1}$  ( $-\text{CH}_2-$  sym. str.), 1675  $\text{cm}^{-1}$  (amide I, C=O str.), 1563  $\text{cm}^{-1}$  (amide II, N-H ben.), 1467  $\text{cm}^{-1}$  ( $-\text{CH}_2-$  scissor).  $^1\text{H}$  NMR (400 MHz,  $\text{CDCl}_3$ ):  $\delta$  0.889 (t, terminal  $-\text{CH}_3$ , 6H), 1.254 (m,  $-\text{CH}_3(\text{CH}_2)_3\text{CH}_2-$ , 52H), 1.429 (m,  $-\text{NHCH}_2\text{CH}_2(\text{CH}_2)_2\text{CH}_2\text{CH}_2\text{NH}-$ , 4H), 1.550–1.575 (m,  $-\text{CH}_3(\text{CH}_2)_{13}\text{CH}_2\text{CH}_2-$  and  $-\text{NHCH}_2\text{CH}_2(\text{CH}_2)_2\text{CH}_2\text{CH}_2\text{NH}-$ , 8H), 3.241–3.320 (m,  $\text{CH}_3(\text{CH}_2)_3\text{CH}_2\text{CH}_2-$  and  $-\text{NHCH}_2(\text{CH}_2)_4\text{CH}_2\text{NH}-$ , 8H), 3.591 (s,  $-\text{CH}_2\text{N}^+(\text{CH}_3)_2\text{CH}_2-$ , 12H), 4.640 (s,  $-\text{CH}_2\text{N}^+(\text{CH}_3)_2\text{CH}_2-$ , 4H), 8.225 (br s,  $\text{CH}_3(\text{CH}_2)_{15}\text{NHCO}-$ , 2H), 8.451 (br s,  $-\text{CONHCH}_2-$ , 2H).  $^{13}\text{C}$  NMR (100 MHz,  $\text{CDCl}_3$ ):  $\delta$  14.220, 22.784, 23.860, 27.150, 29.314, 29.324, 29.440, 29.540, 29.712, 32.422, 38.814, 40.425, 52.925, 64.230, 66.294, 162.758, 163.323. HRMS (ESI)  $m/z$  calculated for  $\text{C}_{50}\text{H}_{102}\text{N}_6\text{O}_4\text{Br}_2$  [M - Br]<sup>+</sup> and [M - 2Br]<sup>2+</sup>: 929.7329, 931.7329, and 425.4073. Found: 929.7130, 931.7121, and 425.4073. Elemental analysis: C 59.48, H 10.19, N 8.33 (calculated); C 59.38, H 10.12, N 8.27 (found).

**Microorganisms and Culture Conditions.** The antibacterial activity of all the small molecular biocides was evaluated against both Gram-positive bacteria (*S. aureus*, MRSA, VRE, and NRSA) and Gram-negative bacteria (*E. coli*, *P. aeruginosa*, *K. pneumonia*, and CREC). *S. aureus*, *P. aeruginosa*, MRSA, *K. pneumonia*, and NRSA were cultured in nutrient broth (5.0 g of peptone, 1.0 g of beef extract, 2.0 g of yeast extract, and 5.0 g of NaCl in 1000 mL of sterile distilled water), while *E. coli* was grown in Luria–Bertani broth (5.0 g of yeast extract, 10.0 g of tryptone, and 10.0 g of NaCl in 1000 mL of sterile distilled water). For VRE brain–heart infusion broth (5.0 g of beef heart infusion form, 12.5 g of calf brain infusion form, 2.5 g of Na<sub>2</sub>HPO<sub>4</sub>, 2.0 g of D-glucose, 10 g of peptone, and 5.0 g of NaCl in 1000 mL of sterile distilled water) was used as growth medium. For solid media, 2.5% agar was used along with the above respective medium. The bacterial freeze-dried stock samples in 30% glycerol were stored at -80 °C. About 5  $\mu\text{L}$  of these stock solutions was added to 3 mL of the respective broth medium, and the cultures were grown for 6 h at 37 °C prior to the antibacterial experiments.

**Antibacterial Assay.** Antibacterial efficacy of all synthesized compounds (4–19) was assayed by the microdilution broth method as described in CLSI guidelines.<sup>51</sup> The 6 h grown culture as described in Microorganism and Culture Conditions gives about 10<sup>9</sup> CFU/mL of bacteria determined by the spread plating method. The bacterial cultures were diluted to give approximately 10<sup>5</sup> CFU/mL in the respective media or buffer and used for determining antibacterial efficacy. All the final compounds except 16–19 were water-soluble at room temperature. Compounds 16–19 were solubilized in water by heating. Stock solutions were prepared by serial dilution of the compounds using sterilized Milli-Q water. The aqueous solutions of serial dilutions (50  $\mu\text{L}$ ) were added to the wells of a 96 well plate followed by the addition of about 150  $\mu\text{L}$  of bacterial suspension (10<sup>5</sup> CFU/mL). The plates were then incubated at 37 °C for 24 h in shaker incubator. The optical density (OD) of the bacterial suspension was recorded using a TECAN (Infinite series, M200 pro) plate reader at 600 nm. Each concentration had triplicate values, the whole experiment was repeated at least twice, and the antibacterial efficacy was determined by taking the average of triplicate OD values for each

concentration and plotting it against concentration. The data was then subjected to sigmoidal fitting. From the curve, the antibacterial activity was determined as the point where the OD value was similar to that of control having no bacteria and expressed as minimum inhibitory concentration (MIC). A glycopeptide antibiotic vancomycin and a lipopeptide colistin were used in this study to compare the antibacterial efficacy.

#### Antibacterial Activity in the Presence of Human Plasma.

Bacteria (*S. aureus*) was grown similarly as mentioned earlier and finally diluted in the respective media to give  $10^5$  CFU/mL. Fresh human blood donated by a healthy donor was centrifuged at 3500 rpm for 5 min. The plasma, which was separated from the blood cells, was carefully collected. The test compound **10** was dissolved in sterile water at a concentration of 2000  $\mu$ g/mL. This was further diluted 2-fold into the plasma so that the final concentration of compound **10** was 1000  $\mu$ g/mL in 50% plasma. Three such test samples were preincubated in 50% plasma for 0, 3, and 6 h, respectively, at 37 °C. Then 50  $\mu$ L of the above solutions was added to wells of a 96-well plate, and 150  $\mu$ L of the bacterial suspension ( $10^5$  CFU/mL) was added to wells containing the test samples in 50% plasma. The plate was then incubated for 24 h at 37 °C, and antibacterial efficacy of the test compound was determined as described above.

#### Antibacterial Activity in Complex Mammalian Fluids.

Blood (sodium heparin as anticoagulant) was donated by healthy human donors. Plasma was isolated by centrifugation of the blood at 3500 rpm for 5 min as mentioned above. Serum was obtained by using SST II Advance serum tube (BD vacutainer) (ref. 367956) containing human blood and then centrifuging the blood at 3500 rpm for 5 min. Methicillin-resistant *S. aureus* (MRSA) was grown similarly as above in nutrient broth for 6 h to give  $\sim 10^9$  CFU/mL. Finally, MRSA was diluted in minimum essential medium (MEM) and mixed with the mammalian systems individually to give  $10^5$  CFU/mL in 50% serum, 50% plasma, and 50% blood supplemented with 50% MEM. The test compound **10** was dissolved in sterile water at a concentration of 4000  $\mu$ g/mL. This was further diluted 2-fold, and then 50  $\mu$ L of the solution was added to wells of a 96-well plate. Bacterial suspension (150  $\mu$ L,  $10^5$  CFU/mL) in 50% serum, 50% plasma, and 50% blood was added individually to the wells containing the test solutions. The plates were then incubated for 24 h at 37 °C, and antibacterial efficacy of the test compound was determined by plating the bacterial suspension (20  $\mu$ L) directly from the wells onto a nutrient agar plate. The agar plates were incubated at 37 °C for 24 h, and colonies were observed to determine the minimum bactericidal concentration (MBC) (the minimum concentration at which the compound killed all the bacterial cells).

#### Bactericidal Time-Kill Assay.

The rate of bactericidal activity, that is, the rate at which the compounds killed bacteria was evaluated by performing time-kill kinetics. Briefly, bacteria (*S. aureus* and *E. coli*) were grown in suitable growth medium at 37 °C for 6 h and diluted in respective media. The compound **10** was added to the bacterial solution (*S. aureus* of approximately  $1.8 \times 10^5$  CFU/mL) at concentrations of MIC and  $6 \times$  MIC in a 96-well plate. The plate was then incubated at 37 °C. At different time intervals (0, 30, 60, 90, 120, 240, and 360 min), 20  $\mu$ L of aliquots from the solution were taken out and serially diluted (10-fold serial dilution) in 0.9% saline. Then 20  $\mu$ L of the dilutions was plated on respective agar plates and incubated at 37 °C for 24 h. The bacterial colonies were counted, and results are represented in logarithmic scale, that is,  $\log_{10}(\text{CFU/mL})$  vs time (in min). A similar experiment was performed with buffer (5 mM HEPES/5 mM glucose = 1:1) with compounds **10** and **18** at 23.6  $\mu$ g/mL against *S. aureus* ( $5.53 \times 10^5$  CFU/mL) and *E. coli* ( $5.03 \times 10^5$  CFU/mL), respectively, at 0, 10, 20, 30, 40, 50, and 60 min time intervals.

#### Biofilm Inhibition Assay.

Midlog phase bacteria (*S. aureus* and *E. coli*, 6 h grown culture) were diluted to a concentration of  $10^5$  CFU/mL in suitable broths supplemented with 1% glucose and NaCl. Compound **10** was serially diluted (2-fold), and 25  $\mu$ L of these serial dilutions was added to the wells of a 96-well plate. Then 75  $\mu$ L of bacterial suspension ( $\sim 10^5$  CFU/mL) was added into the wells containing biocide solutions. A similar experiment was performed by taking 75  $\mu$ L of the bacterial suspension ( $\sim 10^5$  CFU/mL) and 25  $\mu$ L

of sterile water as control. The plates were then incubated under stationary conditions for 24 h. After incubation, the medium was removed and washed a single time with 1× PBS. Then 0.1% crystal violet (CV) solution (100  $\mu$ L) was added into the wells and allowed to incubate for 30 min. Crystal violet solution was then discarded, and the plates were washed with 1× PBS. The residual was solubilized with 200  $\mu$ L of 95% ethanol solution and diluted 10-fold. The OD at 540 nm was then recorded using a plate reader. Biofilm inhibition was quantified by considering 100% biofilm formation in the case of nontreated control.

**Biofilm Disruption Assay.** Bacteria (*S. aureus* and *E. coli*) (6 h grown, midlog phase) were suspended to  $10^5$  CFU/mL into suitable broths (nutrient media supplemented with 1% glucose and NaCl for *S. aureus* and M9 media supplemented with 0.02% casamino acid and 0.5% glycerol for *E. coli*). The well plates containing 100  $\mu$ L of these suspensions were then incubated under stationary conditions (for about 24 h for *S. aureus* and 72 h for *E. coli*). After incubation, the medium was removed and washed with 1× PBS single time. Compound **10** (100  $\mu$ L at various concentrations) was then added to the wells containing established bacterial biofilms and allowed to incubate for 24 h. A control was made where 100  $\mu$ L of medium was added instead of test compound. After 24 h, medium was discarded and planktonic cells were removed by washing with 1× PBS. Then 100  $\mu$ L of trypsin–EDTA solution was added to the treated biofilm to dissolve. Cell suspension of biofilms was then assessed by plating serial 10-fold dilutions on suitable agar plates. After 24 h of incubation, bacterial colonies were counted, and cell viability was expressed as  $\log_{10}(\text{CFU/mL})$  along with the control. For visualizing the disruption of biofilm, 100  $\mu$ L of 0.1% of crystal violet (CV) was added into the wells and incubated for 10 min. Crystal violet solution was then discarded, and the plates were washed once with 1× PBS. Finally, stained wells were imaged using a digital camera.

**Cyttoplasmic Membrane Depolarization Assay.** The 6 h grown bacteria (midlog phase) were harvested (3500 rpm, 5 min), washed in a mixture of 5 mM glucose and 5 mM HEPES buffer (pH = 7.2) (1:1), and resuspended in a mixture of 5 mM HEPES buffer, 5 mM glucose, and 100 mM KCl solution (1:1:1) to give  $\sim 10^8$  CFU/mL. Bacterial suspension (150  $\mu$ L) was added to wells of a 96-well plate (black plate, clear bottom with lid). Then 8  $\mu$ M of 3,3'-dipropylthiadicarbocyanine iodide (diSC<sub>3</sub>5) (50  $\mu$ L) was added to the wells containing bacterial suspension and preincubated for 30 min for *S. aureus* and 60 min for *E. coli* (additional 50  $\mu$ L of 200  $\mu$ M EDTA was also added in the case of *E. coli*). After the incubation, fluorescence was measured for about 8 min at 2 min intervals at an excitation wavelength of 622 nm (slit width = 10 nm) and emission wavelength of 670 nm (slit width = 5 nm). Then, the bacterial suspensions were transferred to another well-plate containing 10  $\mu$ L of 840  $\mu$ g/mL biocides, and fluorescence intensity was monitored similarly for another 12 min. A control experiment was performed by treating the preincubated bacterial and dye solution only with Milli-Q water (10  $\mu$ L).

**Intracellular K<sup>+</sup> Ion Leakage Assay.** The 6 h grown bacteria were harvested (3500 rpm, 5 min), washed, and resuspended in a mixture of 10 mM HEPES buffer and 0.5% glucose (1:1) to give  $\sim 10^8$  CFU/mL. Then 150  $\mu$ L of the bacterial suspension was added into the wells of a 96-well plate (black plate, clear bottom with lid). Then 4  $\mu$ M of PBFI-AM dye (50  $\mu$ L) was added to the wells containing bacterial suspension and preincubated for 30 min for *S. aureus* and 60 min for *E. coli*. After the incubation, fluorescence was measured for about 8 min at 2 min intervals at an excitation wavelength of 346 nm (slit width = 10 nm) and emission wavelength of 505 nm (slit width = 5 nm). Then, the bacterial suspensions were transferred to another well-plate containing 10  $\mu$ L of 840  $\mu$ g/mL biocides, and fluorescence intensity was monitored similarly for another 12 min. Two control experiments were performed by treating the preincubated bacterial and dye solution only with Milli-Q water (10  $\mu$ L) and valinomycin (10  $\mu$ M), respectively, as negative and positive controls.

**Outer Membrane Permeabilization Assay.** Midlog phase *E. coli* cells were harvested (3500 rpm, 4 °C, 5 min), washed, and resuspended in a mixture of 5 mM glucose/5 mM HEPES buffer (1:1) at pH 7.2 to give  $\sim 10^8$  CFU/mL. Bacterial suspension (150  $\mu$ L)

was transferred into the wells of a 96-well plate (black plate, clear bottom with lid). Then 10  $\mu\text{M}$  NPN dye (50  $\mu\text{L}$ ) was added to the wells containing bacterial suspension and preincubated for 60 min. After the incubation, fluorescence was measured for about 8 min at 2 min intervals at excitation wavelength of 350 nm (slit width = 10 nm) and emission wavelength of 420 nm (slit width = 5 nm). Then, the bacterial suspensions were transferred to another well-plate containing 10  $\mu\text{L}$  of 840  $\mu\text{g}/\text{mL}$  biocides, and fluorescence intensity was monitored similarly for another 12 min. A control experiment was performed by treating the preincubated bacterial and dye solution only with Milli-Q water (10  $\mu\text{L}$ ).

**Inner Membrane Permeabilization Assay.** Bacteria (*S. aureus* and *E. coli*, midlog phase) were harvested (3500 rpm, 5 min), washed, and resuspended in a mixture of 5 mM glucose and 5 mM HEPES buffer (pH = 7.2) (1:1). Bacterial suspension (150  $\mu\text{L}$ ) was added to wells of a 96-well plate (black plate, clear bottom with lid). Then 10  $\mu\text{M}$  propidium iodide (PI, 50  $\mu\text{L}$ ) was added to the wells containing bacterial suspension and preincubated for 30 min for *S. aureus* and 60 min for *E. coli*. After the incubation, fluorescence was measured for about 8 min at 2 min intervals at excitation wavelength of 535 nm (slit width = 10 nm) and emission wavelength of 617 nm (slit width = 5 nm). Then, the bacterial suspensions were transferred to another well-plate containing 10  $\mu\text{L}$  of 840  $\mu\text{g}/\text{mL}$  biocides, and fluorescence intensity was monitored similarly for another 12 min. A control experiment was performed by treating the preincubated bacterial and dye solution only with Milli-Q water (50  $\mu\text{L}$ ).

**Resistance Studies.** Propensity to develop bacterial resistance was studied against both *S. aureus* and *E. coli* following a protocol reported earlier.<sup>44,46</sup>

**Hemolytic Activity.** Hemolytic activity of the cationic biocides was studied against human red blood cells (hRBC) following a protocol as published in our earlier reports.<sup>36</sup>

**Cytotoxicity Assay.** Cytotoxicity of the cationic biocides was also studied against human embryonic kidney (HEK) 293 and human cervical carcinoma (HeLa) cells following a protocol as published in our earlier reports.<sup>35,36</sup>

## ■ ASSOCIATED CONTENT

### S Supporting Information

HRMS spectra and HPLC chromatograms with retention time of the molecules, figures showing the MIC values of biocides, activity after incubating in plasma, and activity in complex mammalian fluids, figures showing antibacterial kinetics and hemolytic activity, optical microscopy images of HEK and HeLa cells. The Supporting Information is available free of charge on the ACS Publications website at DOI: 10.1021/acs.jmedchem.Sb00443.

## ■ AUTHOR INFORMATION

### Corresponding Author

\*E-mail: jayanta@jncasr.ac.in. Phone: 080-2208-2565.

### Notes

The authors declare no competing financial interest.

## ■ ACKNOWLEDGMENTS

We thank Prof. C. N. R. Rao, FRS (JNCASR), for his constant support and encouragement. J. Hoque thanks JNCASR for senior research fellowship (SRF). The work was supported by Ramanujan Fellowship (SR/S2/RJN-43/2009 for J. Haldar) from Department of Science and Technology, Government of India. S.S. is grateful to Sheikh Saqr Laboratory (SSL), JNCASR, for postdoctoral fellowship.

## ■ ABBREVIATIONS USED

$\delta$ , chemical shift in parts per million (downfield from tetramethylsilane); EC<sub>50</sub>, half maximal effective concentration;

FT, Fourier transform; HRMS, high-resolution mass spectrometry; HEK, human embryonic kidney; IC<sub>50</sub>, half-maximum inhibitory concentration; IR, infrared; m, multiplet (spectral); *m/z*, mass-to-charge ratio; Me, methyl; MIC, minimal inhibitory concentration; M<sup>+</sup>, parent molecular ion; MRSA, methicillin-resistant *Staphylococcus aureus*; OD, optical density; RBC, red blood cell; rt, room temperature; s, singlet (spectral); t, triplet (spectral)

## ■ REFERENCES

- (1) Taubes, G. The Bacteria Fight Back. *Science* **2008**, *321*, 356–361.
- (2) Walsh, C. Molecular Mechanisms that Confer Antibacterial Drug Resistance. *Nature* **2000**, *406*, 775–781.
- (3) Alekshun, M. N.; Levy, S. B. Molecular Mechanisms of Antibacterial Multidrug Resistance. *Cell* **2007**, *128*, 1037–1050.
- (4) Bush, K.; Courvalin, P.; Dantas, G.; Davies, J.; Eisenstein, B.; Huovinen, P.; Jacoby, G. A.; Kishony, R.; Kreiswirth, B. N.; Kutter, E.; Lerner, S. A.; Levy, S.; Lewis, K.; Lomovskaya, O.; Miller, J. H.; Mobashery, S.; Piddock, L. J. V.; Projan, S.; Thomas, C. M.; Tomasz, A.; Tulkens, P. M.; Walsh, T. R.; Watson, J. D.; Witkowski, J.; Witte, W.; Wright, G.; Yeh, P.; Zgurskaya, H. I. Tackling Antibiotic Resistance. *Nat. Rev. Microbiol.* **2011**, *9*, 894–896.
- (5) Costerton, J. W.; Stewart, P. S.; Greenberg, E. P. Bacterial Biofilms: A Common Cause of Persistent Infections. *Science* **1999**, *284*, 1318–1322.
- (6) Hall-Stoodley, L.; Costerton, W. J.; Stoodley, P. Bacterial Biofilms: from the Natural Environment to Infectious Diseases. *Nat. Rev. Microbiol.* **2004**, *2*, 95–108.
- (7) Flemming, H.-C.; Wingender, J. The Biofilm Matrix. *Nat. Rev. Microbiol.* **2010**, *8*, 623–633.
- (8) Fux, C. A.; Costerton, J. W.; Stewart, P. S.; Stoodley, P. Survival Strategies of Infectious Biofilms. *Trends Microbiol.* **2005**, *13*, 34–40.
- (9) Høiby, N.; Bjarnsholt, T.; Givskov, M.; Molin, S.; Ciofu, O. Antibiotic Resistance of Bacterial Biofilms. *Int. J. Antimicrob. Agents* **2010**, *35*, 322–332.
- (10) Rasmussen, T. B.; Givskov, M. Quorum-sensing Inhibitors as Anti-pathogenic Drugs. *Int. J. Med. Microbiol.* **2006**, *296*, 149–161.
- (11) Davies, D. Understanding Biofilm Resistance to Antibacterial Agents. *Nat. Rev. Drug Discovery* **2003**, *2*, 114–122.
- (12) Parsek, M. R.; Singh, P. K. Bacterial Biofilms: An Emerging Link to Disease Pathogenesis. *Annu. Rev. Microbiol.* **2003**, *57*, 677–701.
- (13) Wagner, V. E.; Iglesias, B. H. P. aeruginosa Biofilms in CF Infection. *Clin. Rev. Allergy Immunol.* **2008**, *35*, 124–134.
- (14) Gomez, M. I.; Prince, A. Opportunistic Infections in Lung Disease: *Pseudomonas* Infections in Cystic Fibrosis. *Curr. Opin. Pharmacol.* **2007**, *7*, 244–251.
- (15) Bjarnsholt, T.; Ciofu, O.; Molin, S.; Givskov, M.; Høiby, N. Applying Insights from Biofilm Biology to Drug Development—Can a New Approach be Developed? *Nat. Rev. Drug Discovery* **2013**, *12*, 791–808.
- (16) Arciola, C. R.; Campoccia, D.; Speziale, P.; Montanaro, L.; Costerton, J. W. Biofilm Formation in *Staphylococcus* Implant Infections. A Review of Molecular Mechanisms and Implications for Biofilm-Resistant Materials. *Biomaterials* **2012**, *33*, 5967–5982.
- (17) Warren, J. W. Catheter-Associated Urinary Tract Infections. *Int. J. Antimicrob. Agents* **2001**, *17*, 299–303.
- (18) Zasloff, M. Antimicrobial Peptides of Multicellular Organisms. *Nature* **2002**, *415*, 389–395.
- (19) Donadio, S.; Maffioli, S.; Monciardini, P.; Sosio, M.; Jabes, D. Antibiotic Discovery in the Twenty-first Century: Current Trends and Future Perspectives. *J. Antibiot.* **2010**, *63*, 423–430.
- (20) Hancock, R. E. W.; Sahl, H.-G. Antimicrobial and Host-defense Peptides as New Anti-infective Therapeutic Strategies. *Nat. Biotechnol.* **2006**, *24*, 1551–1557.
- (21) Straus, S. K.; Hancock, R. E. W. Mode of Action of the New Antibiotic for Gram-positive Pathogens Daptomycin: Comparison with Cationic Antimicrobial Peptides and Lipopeptides. *Biochim. Biophys. Acta, Biomembr.* **2006**, *1758*, 1215–1223.

- (22) Luca, V.; Stringaro, A.; Colone, M.; Pini, A.; Mangoni, M. L. Esculentin(1–21), an Amphibian Skin Membrane-active Peptide with Potent Activity on both Planktonic and Biofilm Cells of the Bacterial Pathogen *Pseudomonas aeruginosa*. *Cell. Mol. Life Sci.* **2013**, *70*, 2773–2786.
- (23) Bionda, N.; Pastar, I.; Davis, S. C.; Cudic, P. In Vitro and in Vivo Activities of Novel Cyclic Lipopeptides against Staphylococcal Biofilms. *Protein Pept. Lett.* **2014**, *21*, 352–356.
- (24) Chen, Y. X.; Mant, C. T.; Farmer, S. W.; Hancock, R. E. W.; Vasil, M. L.; Hodges, R. S. Rational Design of Alpha-helical Antimicrobial Peptides with Enhanced Activities and Specificity/Therapeutic Index. *J. Biol. Chem.* **2005**, *280*, 12316–12329.
- (25) Porter, E. A.; Wang, X.; Lee, H. S.; Weisblum, B.; Gellman, S. H. Non-haemolytic Beta Amino-acid Oligomers. *Nature* **2000**, *405*, 298–298.
- (26) Radzishevsky, I. S.; Rotem, S.; Bourdetsky, D.; Navon-Venezia, S.; Carmeli, Y.; Mor, A. Improved Antimicrobial Peptides based on Acyl-lysine Oligomers. *Nat. Biotechnol.* **2007**, *25*, 657–659.
- (27) Tang, H.; Doerkson, R. J.; Tew, G. N. Synthesis of Urea Oligomers and their Antibacterial Activity. *Chem. Commun.* **2005**, *28*, 1537–1539.
- (28) Liu, D. H.; Choi, S.; Chen, B.; Doerkson, R. J.; Clements, D. J.; Winkler, J. D.; Klein, M. L.; DeGrado, W. F. Nontoxic Membrane-active Antimicrobial Arylamide Oligomers. *Angew. Chem., Int. Ed.* **2004**, *43*, 1158–1162.
- (29) Thaker, H. D.; Som, A.; Ayaz, F.; Lui, D.; Pan, W.; Scott, R. W.; Anguita, J.; Tew, G. N. Synthetic Mimics of Antimicrobial Peptides with Immunomodulatory Responses. *J. Am. Chem. Soc.* **2012**, *134*, 11088–11091.
- (30) Nederberg, F.; Zhang, Y.; Tan, J. P. K.; Xu, K. J.; Wang, H. Y.; Yang, C.; Gao, S. J.; Guo, X. D.; Fukushima, K.; Li, L. J.; Hedrick, J. L.; Yang, Y. Y. Biodegradable Nanostructures with Selective Lysis of Microbial Membranes. *Nat. Chem.* **2011**, *3*, 409–414.
- (31) Uppu, D. S. S. M.; Akkapeddi, P.; Manjunath, G. B.; Yarlagadda, V.; Hoque, J.; Haldar, J. Polymers with Tunable Side-chain Amphiphilicity as Non-hemolytic Antibacterial Agents. *Chem. Commun.* **2013**, *49*, 9389–9391.
- (32) Chongsiriwatana, N. P.; Patch, J. A.; Czyzewski, A. M.; Dohm, M. T.; Ivankin, A.; Gidalevitz, D.; Zuckermann, R. N.; Barron, A. E. Peptoids that Mimic the Structure, Function, and Mechanism of Helical Antimicrobial Peptides. *Proc. Natl. Acad. Sci. U. S. A.* **2008**, *105*, 2794–2799.
- (33) Haug, B. E.; Stensen, W.; Kalaaji, M.; Rekdal, O.; Svendsen, J. S. Synthetic Antimicrobial Peptidomimetics with Therapeutic Potential. *J. Med. Chem.* **2008**, *51*, 4306–4314.
- (34) Goodman, C. M.; Choi, S.; Shandler, S.; DeGrado, W. F. Foldamers as Versatile Frameworks for the Design and Evolution of Function. *Nat. Chem. Biol.* **2007**, *3*, 252–262.
- (35) Ghosh, C.; Manjunath, G. B.; Akkapeddi, P.; Yarlagadda, V.; Hoque, J.; Uppu, D. S. S. M.; Konai, M. M.; Haldar, J. Small Molecular Antibacterial Peptoid Mimics: The Simpler the Better! *J. Med. Chem.* **2014**, *57*, 1428–1436.
- (36) Konai, M. M.; Ghosh, C.; Yarlagadda, V.; Samaddar, S.; Haldar, J. Membrane Active Phenylalanine Conjugated Lipophilic Norspermidine Derivatives with Selective Antibacterial Activity. *J. Med. Chem.* **2014**, *57*, 9409–9423.
- (37) Hoque, J.; Akkapeddi, P.; Yarlagadda, V.; Uppu, D. S. S. M.; Kumar, P.; Haldar, J. Cleavable Cationic Antibacterial Amphiphiles: Synthesis, Mechanism of Action, and Cytotoxicities. *Langmuir* **2012**, *28*, 12225–12234.
- (38) Lister, P. D.; Wolter, D. J.; Hanson, N. D. Antibacterial-Resistant *Pseudomonas aeruginosa*: Clinical Impact and Complex Regulation of Chromosomally Encoded Resistance Mechanisms. *Clin. Microbiol. Rev.* **2009**, *22*, 582–610.
- (39) DeMarco, C. E.; Cushing, L. A.; Frempong-Manso, E.; Seo, S. M.; Jaravaza, T. A. A.; Kaatz, G. W. Efflux-Related Resistance to Norfloxacin, Dyes, and Biocides in Bloodstream Isolates of *Staphylococcus aureus*. *Antimicrob. Agents Chemother.* **2007**, *51*, 3235–3239.
- (40) Urban, C.; Tiruvury, H.; Mariano, N.; Colon-Urban, R.; Rahal, J. J. Polymyxin-Resistant Clinical Isolates of *Escherichia coli*. *Antimicrob. Agents Chemother.* **2011**, *55*, 388–389.
- (41) Choi, H.; Chakraborty, S.; Liu, R.; Gellman, S. H.; Weisshaar, J. C. *PLoS One* **2014**, *9*, e104500.
- (42) Ge, Y.; MacDonald, D. L.; Holroyd, K. J.; Thornsberry, C.; Wexler, H.; Zasloff, M. In Vitro Antibacterial Properties of Pexiganan, an Analog of Magainin. *Antimicrob. Agents Chemother.* **1999**, *43*, 782–788.
- (43) Sambhy, V.; MacBride, M. M.; Peterson, B. R.; Sen, A. Silver Bromide Nanoparticle/Polymer Composites: Dual Action Tunable Antimicrobial Materials. *J. Am. Chem. Soc.* **2006**, *128*, 9798–9808.
- (44) Rogers, S. A.; Huigens, R. W., III; Melander, C. A 2-Aminobenzimidazole That Inhibits and Disperses Gram-Positive Biofilms through a Zinc-Dependent Mechanism. *J. Am. Chem. Soc.* **2009**, *131*, 9868–9869.
- (45) Hu, Y.; Amin, M. N.; Padhee, S.; Wang, R. E.; Qiao, Q.; Bai, G.; Li, Y.; Mathew, A.; Cao, C.; Cai, J. Lipidated Peptidomimetics with Improved Antimicrobial Activity. *ACS Med. Chem. Lett.* **2012**, *3*, 683–686.
- (46) Yarlagadda, V.; Akkapeddi, P.; Manjunath, G. B.; Haldar, J. Membrane Active Vancomycin Analogs: A Strategy to Combat Bacterial Resistance. *J. Med. Chem.* **2014**, *57*, 4558–4568.
- (47) Makovitzki, A.; Avrahami, D.; Shai, Y. Ultrashort Antibacterial and Antifungal Lipopeptides. *Proc. Natl. Acad. Sci. U. S. A.* **2006**, *103*, 15997–16002.
- (48) Hoque, J.; Akkapeddi, P.; Yadav, V.; Manjunath, G. B.; Uppu, D. S. S. M.; Konai, M. M.; Yarlagadda, V.; Sanyal, K.; Haldar, J. Broad Spectrum Antibacterial and Antifungal Polymeric Paint Materials: Synthesis, Structure-Activity Relationship, and Membrane-Active Mode of Action. *ACS Appl. Mater. Interfaces* **2015**, *7*, 1804–1815.
- (49) Ilker, M. F.; Nüsslein, K.; Tew, G. N.; Coughlin, E. B. Tuning the Hemolytic and Antibacterial Activities of Amphiphilic Polynorbornene Derivatives. *J. Am. Chem. Soc.* **2004**, *126*, 15870–15875.
- (50) Niu, Y.; Padhee, S.; Wu, H.; Bai, G.; Qiao, Q.; Hu, Y.; Harrington, L.; Burda, W. N.; Shaw, L. N.; Cao, C.; Cai, J. Lipo- $\gamma$ -AApeptides as a New Class of Potent and Broad-Spectrum Antimicrobial Agents. *J. Med. Chem.* **2012**, *55*, 4003–4009.
- (51) Wiegand, I.; Hilpert, K.; Hancock, R. E. W. Agar and Broth Dilution Methods to Determine the Minimal Inhibitory Concentration (MIC) of Antimicrobial Substances. *Nat. Protoc.* **2008**, *3*, 163–175.